AFRL-RQ-WP-TR-2015-0141

DYNAMIC STABILITY DERIVATIVES

Jerry E. Jenkins

Aerodynamic Technology Branch
Aerospace Vehicles Division

JUNE 2015
Interim Report

AIR FORCE RESEARCH LABORATORY
AEROSPACE SYSTEMS DIRECTORATE
WRIGHT-PATTERSON AIR FORCE BASE, OH 45433-7541
AIR FORCE MATERIEL COMMAND
UNITED STATES AIR FORCE

NOTICE AND SIGNATURE PAGE

Using Government drawings, specifications, or other data included in this document for any purpose other than Government procurement does not in any way obligate the U.S. Government. The fact that the Government formulated or supplied the drawings, specifications, or other data does not license the holder or any other person or corporation; or convey any rights or permission to manufacture, use, or sell any patented invention that may relate to them.

This report was cleared for public release by the USAF 88th Air Base Wing (88 ABW) Public Affairs Office (PAO) and is available to the general public, including foreign nationals.

Copies may be obtained from the Defense Technical Information Center (DTIC) (http://www.dtic.mil).

AFRL-RQ-WP-TR-2015-0141 HAS BEEN REVIEWED AND IS APPROVED FOR PUBLICATION IN ACCORDANCE WITH ASSIGNED DISTRIBUTION STATEMENT.

*//Signature//
MICHAEL V. OL
Project Engineer and Technical Advisor
Aerodynamic Technology Branch
Aerospace Vehicles Division
Aerospace Systems Directorate

//Signature//
MOLLIE C. ESCHEL
Deputy Branch Chief
Aerodynamic Technology Branch
Aerospace Vehicles Division
Aerospace Systems Directorate

This report is published in the interest of scientific and technical information exchange, and its publication does not constitute the Government's approval or disapproval of its ideas or findings.

*Disseminated copies will show "//Signature//" stamped or typed above the signature blocks.

REPORT DOCUMENTATION PAGE

Form Approved
OMB No. 0704-0188

1. REPORT DATE *(DD-MM-YY)*	2. REPORT TYPE	3. DATES COVERED *(From - To)*
June 2015	Interim	01 June 2014 – 30 November 2014

4. TITLE AND SUBTITLE
DYNAMIC STABILITY DERIVATIVES

5a. CONTRACT NUMBER
In-house

5b. GRANT NUMBER

5c. PROGRAM ELEMENT NUMBER
N/A

6. AUTHOR(S)
Jerry E. Jenkins (AFRL/RQVA Emeritus)

5d. PROJECT NUMBER
N/A

5e. TASK NUMBER
N/A

5f. WORK UNIT NUMBER
N/A

7. PERFORMING ORGANIZATION NAME(S) AND ADDRESS(ES)
Aerodynamic Technology Branch (AFRL/RQVA)
Aerospace Vehicles Division
Air Force Research Laboratory, Aerospace Systems Directorate
Wright-Patterson Air Force Base, OH 45433-7541
Air Force Materiel Command, United States Air Force

8. PERFORMING ORGANIZATION REPORT NUMBER
AFRL-RQ-WP-TR-2015-0141

9. SPONSORING/MONITORING AGENCY NAME(S) AND ADDRESS(ES)
Air Force Research Laboratory
Aerospace Systems Directorate
Wright-Patterson Air Force Base, OH 45433-7541
Air Force Materiel Command
United States Air Force

10. SPONSORING/MONITORING AGENCY ACRONYM(S)
AFRL/RQVA

11. SPONSORING/MONITORING AGENCY REPORT NUMBER(S)
AFRL-RQ-WP-TR-2015-0141

12. DISTRIBUTION/AVAILABILITY STATEMENT
Approved for public release; distribution unlimited.

13. SUPPLEMENTARY NOTES
PA Case Number: 88ABW-2015-0574; Clearance Date: 17 Feb 2015. This is a work of the U.S. Government and is not subject to copyright protection in the United States.

14. ABSTRACT
Measurement and interpretation of dynamic stability derivatives are examined in the context of Aerodynamic Modeling (the technical discipline that deals with representing vehicle aerodynamic responses in a mathematical form consistent with the analyst's needs). Several such techniques are discussed with emphasis on the classic stability derivative approach. Importantly, complications imposed by unsteady aerodynamic responses (those in which the forces and/or moments cannot be taken as simply related to the aircraft's instantaneous motion state) are considered. Furthermore, the implications of using wind-tunnel dynamic testing equipment that cannot isolate the effects of particular motion variables are addressed.

The stability derivative concept is still the most widely used aerodynamic modeling technique and is based on two fundamental assumptions: 1) instantaneous aerodynamic loads depend only on the instantaneous values of the motion variables; and 2) they vary linearly with the motion variables. However, these assumptions prohibit a precise representation of unsteady aerodynamic responses to an arbitrary motion input. Specifically, stability "derivatives" with respect to the rates-of-change of the state variables are shown to be terms of an asymptotic expansion of the aerodynamic response to an arbitrary motion input. Therefore they are valid only in the limit as the non-dimensional motion rates approach zero. The insight gained from adopting this point of view is shown to be useful in laying out an experimental program and interpreting the results.

Discussions of dynamic testing techniques in the wind tunnel; data reduction methodology; assessment of the validity of the resulting dynamic derivative model; and means for properly expressing measured stability derivatives with respect to the desired flight dynamics coordinate system are provided.

15. SUBJECT TERMS dynamic stability derivatives, dynamic wind tunnel testing techniques

16. SECURITY CLASSIFICATION OF:			17. LIMITATION OF ABSTRACT:	18. NUMBER OF PAGES	19a. NAME OF RESPONSIBLE PERSON (Monitor)
a. REPORT	b. ABSTRACT	c. THIS PAGE			Michael V. Ol
Unclassified	Unclassified	Unclassified	SAR	59	19b. TELEPHONE NUMBER *(Include Area Code)* N/A

Table of Contents

1 Introduction

We begin with a brief overview of the design process. Its purpose is to establish the need for mathematical models relating an air vehicle's motion and its aerodynamic loads. This is followed by a discussion of several aerodynamic modeling techniques with emphasis on the classic stability derivative approach. Importantly, requirements imposed by unsteady aerodynamic responses (those in which the forces and/or moments cannot be taken as simply related to the aircraft's instantaneous motion state) are considered. Finally, the report concludes with discussions of dynamic testing techniques in the wind tunnel; data reduction methodology; ways to assess the validity of the resulting dynamic derivative model; and means for properly expressing measured stability derivatives with respect to the desired flight dynamics coordinate system.

1.1 Performance vs. Stability and Control Analyses

Performance assessments generally involve the prediction of a maximum (or minimum) value for a steady-state parameter. Range, top speed, normal acceleration and turning radius are typical. Even when flight trajectories are needed (e.g., take-off distance to clear a 50 foot obstacle) the aircraft's rotational degrees of freedom are seldom considered. In the latter case, angle-of-attack variations can be considered to be an "input" and the analyst is looking for the optimum time history that minimizes take-off distance. As a consequence, the primary aerodynamic characteristics of interest are the lift and drag forces as a function of angle of attack. Vehicle weight is the only mass property of interest.

On the other hand, stability and control analyses involve the time-history of the aircraft's motion in response to control surface deflections, atmospheric disturbances, store release, etc. Vehicle steady-state responses in all six degrees of freedom are crucial to the result as are the transient responses following the input. This requires knowledge of all the aircraft's mass properties (including moments of inertia and center-of-gravity location). Furthermore, the aerodynamic characteristics (all of the forces and moments) must be understood as time-varying quantities that depend on the resulting motion (which itself is unknown a priori).

The aircraft is a set of integrated systems, each designed to provide functions dictated by mission requirements. However, for the most part, these systems should not be designed independently of each other. "Murphy" guarantees that requirements placed on one or more of the subsystems will inevitably impose restrictions (sometimes severe) on at least one other subsystem. As suggested in Figure 1-1, compromised aerodynamic characteristics (perhaps for increased performance or reduced observables) often require an automatic control system to provide acceptable handling and/or ride qualities. Even without compromises imposed by other systems, a flight control system may be required to obtain good handling qualities throughout the flight envelope.

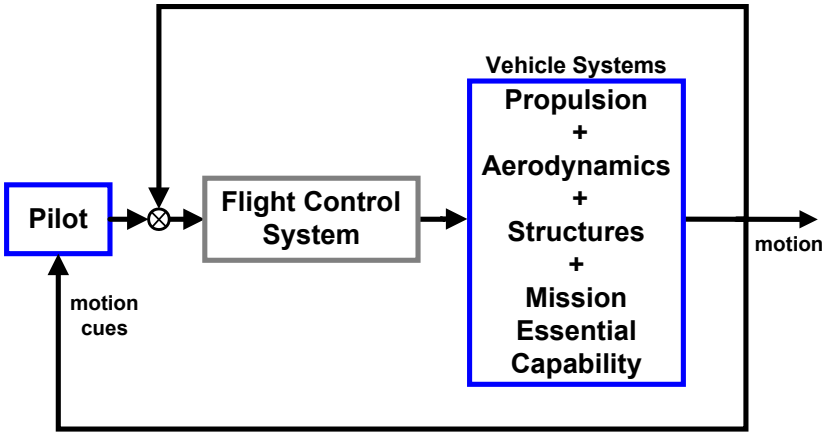

Figure 1-1

Note that the pilot's ability to perform a specific task not only depends on the vehicle's dynamic response characteristics but on the manner in which he/she is provided with motion cues or other mission related information.

Clearly, if design activities are to be efficient, mathematical models of the evolving systems must be sufficiently accurate, amenable to rapid turn-around, and in a form that permits the determination of system parameters. Early in the design phase one may accept relatively crude approximations, with model sophistication increasing as the design progresses.

As the subsystem designs mature, their performance (especially when interacting) needs to be evaluated. Thus, mathematical models, suitable for simulation, are also required. Many simulations, by the very nature of the systems being evaluated, ***must operate in real time*** (pilot-in-the-loop handling qualities, for example). This has important implications regarding acceptable forms for aerodynamic reaction models.

1.2 The Aerodynamic "Subsystem"

Figure 1-2 offers a closer look at the elements comprising the aerodynamic subsystem. For simulations, one could consider using the fluid-dynamic equations (which are partial differential equations) as the aerodynamic model, coupling them with the equations of motion, and solving them "on-line." Getting sufficient accuracy without going to the full Navier-Stokes equations is an issue and there is little hope that such a simulation could run in real time.

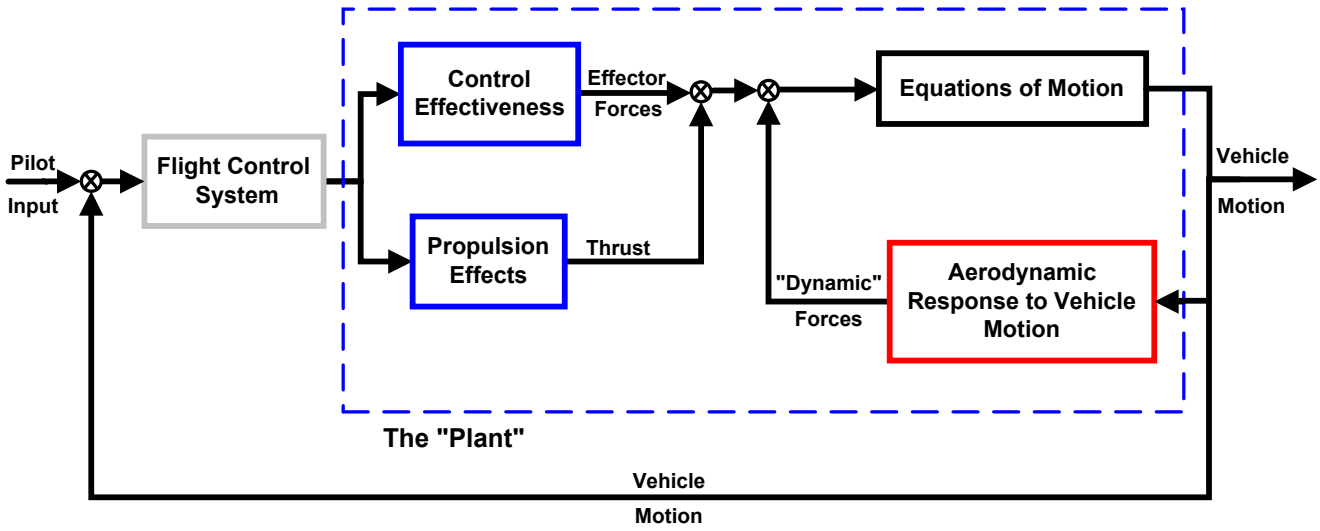

Figure 1-2 - Aerodynamic Subsystem

Although models are clearly needed for the suite of control devices and for propulsion effects in the presence of airframe components (blue blocks in Figure 1-2), our attention is restricted to the aerodynamic response of the air-vehicle to motion inputs (red block). Newton took care of the equations of motion; we see no need to improve on his work.

All system elements are represented in terms of "black-box" input-output relationships. In our case, the inputs are specific aircraft motion variables and the outputs are the resulting aerodynamic forces and moments. (For the control effectiveness and propulsion blocks, the inputs would be pilot "stick" and throttle commands, perhaps modified by the flight control system). Thus, it is natural to consider treating the aerodynamics in the same way that one would treat ***any*** dynamic system, using appropriate techniques from the system theory "tool kit." In doing so, those characteristics unique to fluid-dynamic "systems" must be honored.

We should also note that the use of an automatic control system to provide adequate system dynamics does not get us off the hook. The plant (as the control-theory people like to call it) being controlled is defined by the elements inside the dashed box. An optimal flight control system design requires an accurate plant description. Robust control systems (i.e. ones that are insensitive to uncertainties in the plant model) can be designed. However, this almost always comes at the requires increased control effectiveness and/or control power requirements which in turn affect actuator sizing, structural integrity and the overall aerodynamic design (Murphy strikes again).

2 Aerodynamic Modeling

Aerodynamic Modeling is the technical discipline that deals with representing vehicle aerodynamic responses in a mathematical form consistent with the analyst's needs.

2.1 Essential Model Characteristics

Of course, the simplest possible aerodynamic model is desired for a variety of reasons. Obviously, the power and efficiency of linear analysis and/or synthesis procedures must ***not*** be discarded unnecessarily. Still, mathematical representations used to describe the aerodynamic response must provide valid results; i.e., predicted vehicle motions must accurately portray full-scale behavior. In all cases, the following conditions must be met:

(1) Aerodynamic models must be expressed in a form that is applicable to arbitrary motions. This means that they must depend explicitly ***only on the vehicle state variables*** (the dependent variables in the equations of motion) ***and possibly time***. For example, a model determined from a set of harmonic motion data must contain ***no explicit dependency*** on frequency or amplitude, since these parameters have no meaning in the context of more general motions nor do they appear as state variables in the equations of motion.

(2) Aerodynamic models must accurately describe the aircraft's behavior. Notably: static discontinuities, multiple time scales (including large time lags), and motion history effects must be included when present.

(3) Clearly, aerodynamic responses must be modeled in a manner consistent with the physical phenomena that cause them; i.e., their mathematical form should be derivable from first principles. This implies that a systematic simplification (consistent with the aerodynamic response and the motion being studied) of more general mathematical models must yield the conventional (i.e., widely accepted) representations.

An approach consistent with these requirements is illustrated in Figure 2-1, adapted from Reference 1.

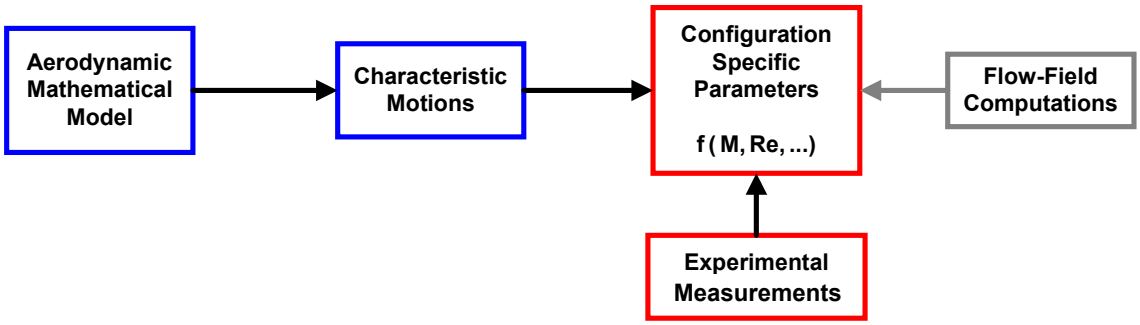

Figure 2-1 - Aerodynamic Modeling Approach

The idea is to start with a mathematical representation for the aerodynamic reaction (to a motion input) which is general enough to accurately capture the essential features of the output force/moment ***for the vehicle and flight regime of interest***. This mathematical model is an appropriately chosen relationship from dynamic system theory (more on that later). Also a limited number of "characteristic motions" must be chosen, from which ***arbitrary*** vehicle motions (i.e., unspecified *a priori*) can be constructed. The total response consists of the superposition of many individual characteristic motions implying that each must be the response to a sufficiently small perturbation.

Model parameters can then be "identified" from a well-designed wind tunnel experiment (consisting of an appropriate set of characteristic motions). Of course, numerical "experiments" could be used in lieu of wind tunnel tests, but the procedure is essentially the same. Provided that suitable selections for mathematical model form ***and for*** the characteristic motion set are made, the resulting configuration specific model can accurately represent the aerodynamic response for arbitrary motions. If

either of these conditions is ***not*** met, the result is little more than a "curve fit" that may or may not yield good results when applied to motions not included in the test matrix.

2.2 Stability Derivatives - Bryan's Model (1911)

In 1911, Bryan[2] introduced the stability derivative concept, and it is still the most widely used aerodynamic modeling technique. His work was based on two fundamental assumptions[1]:

(1) Instantaneous aerodynamic loads depend ***only on the instantaneous values*** of the motion variables

(2) They ***vary linearly*** with the motion variables.

The first assumption allows the expression of an aerodynamic response as a ***function*** of the motion variable(s) and the second permits the Taylor series expansion (of the function) about some reference point, retaining only the linear terms of the expansion. Thus for the lift response to a pitch-plane motion input we may write:

$$L(\alpha,q,t) = L(\alpha_0) + \Delta\alpha(t)\left(\frac{\partial L}{\partial \alpha}\right)_{\substack{\alpha=\alpha_0 \\ q=0}} + q(t)\left(\frac{\partial L}{\partial q}\right)_{\substack{\alpha=\alpha_0 \\ q=0}}$$

where:

The partial derivative with respect to α is the dimensional form of the lift vs. angle-of-attack stability derivative L_α; i.e., the static lift-curve slope.

and

the partial derivative with respect to q is the dimensional form of the lift vs. pitch-rate stability derivative L_q.

In Bryan's formulation, ***each stability derivative*** appearing in the expansion ***is time-invariant*** and therefore is to be evaluated from a ***steady-flow*** condition while holding all other inputs constant at the reference flight condition, α_0. This poses no difficulty since it's entirely possible to fly at constant angle of attack with a non-zero pitch rate; e.g., a constant "g" pull-up or a steady-state turn.

However, there is no justification, under Bryan's first assumption, for including derivatives with respect to the rate(s)-of-change of the motion variable(s), in this case either $\dot{\alpha}$ or $\dot{q}$. Derivatives accounting for the rate-of-change of a motion variable are necessarily associated with a time-dependent, i.e., unsteady, flow field. (How can $\dot{\alpha}$ and/or $\dot{q}$ be non-zero for any appreciable time interval while α and/or q remain constant?) ***Nevertheless, experience has shown that such terms are necessary when significant lags are present in the aerodynamic response, e.g., the time lag required for changes in wing downwash to reach a horizontal tail.***[1]

We will return to this issue later. However as a starting point, the lift response to an angle-of-attack input is derived in the usual manner; i.e., the change in lift from a reference flight condition is given by a Taylor series expansion of the vehicle motion followed by a second Taylor expansion in terms of the motion variables and their time derivatives.

Thus, an expansion of the function describing the angle-of-attack time-history allows us to write:

$$\alpha(t) = \alpha_0 + \dot{\alpha}_0 t + \frac{1}{2}\ddot{\alpha}_0 t^2 + \cdots$$

Successive differentiation yields

$$\dot{\alpha}(t) = \dot{\alpha}_0 + \ddot{\alpha}_0 t + \cdots$$

$$\ddot{\alpha}(t) = \ddot{\alpha}_0 + \cdots$$

Therefore, given an expression for the lift response due to an arbitrary input,

$$L(t) = f_1(\alpha(t), t)$$

Substitution for $\alpha(t)$, and subsequent rearrangement (using the motion derivatives as needed), allows the lift equation to be put in the form:

$$L(t) = f_2\left(\alpha(t),\, \dot{\alpha}(t),\, \ddot{\alpha}(t), \cdots, t\right)$$

After substituting for $\alpha(t)$ and its derivatives, there may be functions of t "left over" that cannot be eliminated. These will disappear in the next step, a Taylor expansion of this equation (retaining only linear terms):

$$L(t) = \alpha(t)\left(\frac{\partial L}{\partial \alpha}\right)_{\substack{\alpha=\alpha_0 \\ \dot{\alpha}=0 \\ \ddot{\alpha}=0}} + \dot{\alpha}(t)\left(\frac{\partial L}{\partial \dot{\alpha}}\right)_{\substack{\alpha=\alpha_0 \\ \dot{\alpha}=0 \\ \ddot{\alpha}=0}} + \ddot{\alpha}(t)\left(\frac{\partial L}{\partial \ddot{\alpha}}\right)_{\substack{\alpha=\alpha_0 \\ \dot{\alpha}=0 \\ \ddot{\alpha}=0}} + \cdots$$

Each stability derivative (the partial derivatives in this equation) is independent of time; i.e., is evaluated at the steady-state reference flight condition.

However, this derivation provides no definitive information about limits of applicability and leaves several crucial questions unanswered. We have a vague notion that the lift should be a linear function of the motion variables and their time derivatives (at least for small perturbations) and that the two Taylor series expansions need to be convergent. Furthermore, what does the derivative with respect to the angle of attack's rate of change mean in physical terms? Why should we expect the aerodynamic response to vary linearly with this motion parameter?

There is no problem with an expansion of the steady-state lift-curve function in terms of angle of attack and pitch rate. If the lift curve is smooth in the angle-of-attack range of interest, convergence of its Taylor series representation is assured. However, as indicated above, a Taylor series expansion of the motion-history function has problems.

Fortunately, there is a much better way of thinking about the stability derivative model that also provides a better physical feel for the dynamic derivatives. A dimensional analysis sheds some light on the problem. It also identifies the relevant a similarity parameters for efficient dynamic testing.

2.3 Non-dimensional Time – Convection

Consider a three-dimensional straight-tapered wing in unsteady flow. Assume that the lift is defined by a function that depends on properties of the fluid (density, kinematic viscocity, and speed-of-sound); wing geometric characteristics (area, mean aerodynamic chord and taper ratio); and its motion (free-stream velocity, the vehicle's orientation with respect to the free-stream, and its rate-of-change). Time is included since the flow is unsteady.

$$L(t) = f(\rho, \upsilon, a, S, \bar{c}, \lambda_r, U_\infty, \alpha(t), \dot{\alpha}(t), t)$$

A dimensional analysis[3] of the lift relation identifies seven **independent** dimensionless variables.

$$\frac{L(t)}{\frac{1}{2}\rho U_\infty{}^2 S} = C_L(t) = f\left(R_n, M, A, M, \lambda_r, \alpha, \frac{\dot{\alpha}\bar{c}}{2U_\infty}, t\left(\frac{2U_\infty}{\bar{c}}\right)\right)$$

where:

R_n - Reynolds number based on $\bar{c}$
M - Mach number
A - wing aspect ratio

Provided that our list of physical variables is complete, the instantaneous lift coefficient is uniquely determined by the seven ***non-dimensional groupings***. However, since we are representing the time history of angle of attack by a Taylor series expansion, a limited motion-history range is implied since the expansion has been truncated after just two terms. The list of independent variables is incomplete in this sense.

It should come as no surprise that the wing's unsteady lift is represented most efficiently in terms of Reynolds number, Mach number, aspect ratio, taper ratio and angle of attack. However, an inspection of the remaining independent variables is instructive. $\frac{\bar{c}}{2U_\infty}$ is the time required for a fluid "element" (traveling with the free-stream) to be carried a distance equal to one-half the wing's mean aerodynamic chord. That is, it is a measure of the convection speed of the flow relative to a representative longitudinal distance. Thus, time is measured in terms of the number of semi-chords that the free-stream element has traveled.

Looking now at the non-dimensional $\dot{\alpha}$ term, the motion's rate of change is not sufficient to completely describe the unsteady behavior. Rather, the important consideration is the motion's rate of change compared to the time required for the fluid to travel over a representative aircraft length. For **harmonic motio**n, we could have used frequency (ω) in place of $\dot{\alpha}$ as a fundamental physical quantity, since they are intimately related. The result is similar (both have the dimensions sec.^{-1}), i.e., the non-dimensional form of frequency is $k = \dfrac{\omega \bar{c}}{2U_\infty}$ and is called the reduced frequency.

The possibility that flow perturbations convecting downstream can alter the dynamic response must be taken into account. Reduced frequency (or $\dfrac{\dot{\alpha} \bar{c}}{2U_\infty}$) is an important similarity parameter (along with Reynolds number, Mach number, and dynamic pressure) for dynamic testing. Either is a measure of the degree of unsteadiness expected in the response, i.e., it compares the change in angle-of attack (over a given time interval) to the distance downstream that a free-stream perturbation travels in the same interval.

2.4 Unsteady Aerodynamic Responses

A maneuvering aircraft's time-dependent aerodynamic forces are dictated by the history of its motion because of vorticity left in the wake[4]. Consider the unsteady lift response of a thin airfoil. The classical linear theory describing this behavior was derived assuming two-dimensional inviscid flow and an incompressible fluid.[5] Therefore, the theory is applicable for ***small angles of attack and attached flow***. A cambered "thin" airfoil, with a time-varying angle-of-attack input, is shown in Figure 2-2. As for the steady flow case, its lift is directly proportional to the (instantaneous) circulation about the airfoil.

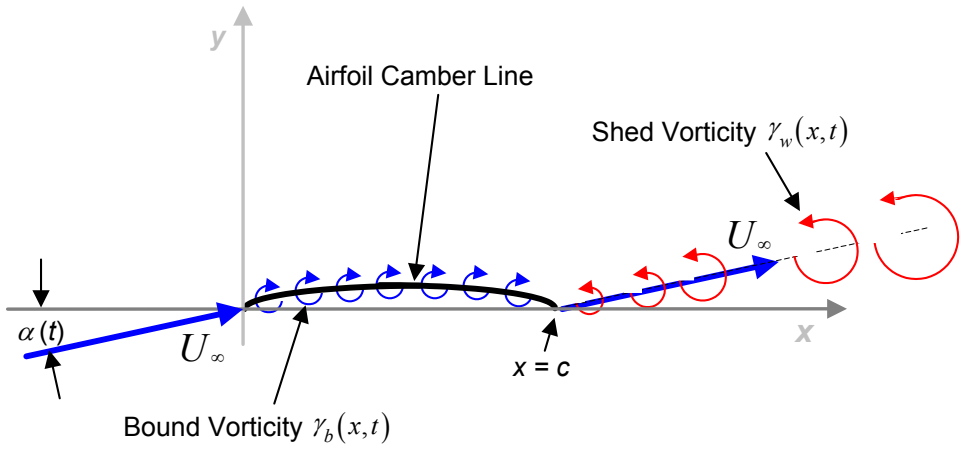

Figure 2-2 - Thin Airfoil in Unsteady Flow

However, a time-varying lift requires that the changing "bound" vorticity (on the airfoil surface) be continually balanced by the shedding of vortex elements into the wake, since by Kelvin's theorem ***the net vorticity must remain constant in an inviscid fluid****, i.e., for all times, the integral of the bound vorticity on the airfoil plus the net vorticity in the wake is a constant,

$$\int_0^c \gamma_b(x,t)\,dx + \int_c^\infty \gamma_w(x,t)\,dx = \text{constant} \qquad \textbf{2-1}$$

The wake consists of a vortex sheet, the "elements" of which are assumed to be traveling downstream at the free-stream velocity. At time t, the strength of the vortex element being shed at the airfoil's trailing edge can be determined by differentiating Equation 2-1, as shown in Figure 2-3. Furthermore, the wake-vortex element shed at time τ is at a point

*In the steady-state case, vorticity on the airfoil is balanced by a single "starting vortex" located infinitely far downstream

$x = c + U_\infty (t - \tau)$ downstream. Thus, ***both*** the ***strengths*** of wake-vortex elements and their ***spatial distribution*** are determined by the time-history of the bound vorticity (a function of the airfoil's prior motion).

Also, as suggested in Figure 2-3, the combined effects of the wake and bound vorticity distributions determine the flow velocity at the airfoil surface (which must be tangent to the surface in potential flow). Note that, according to the Biot-Savart Law, in two-dimensional flow, the wake-vortex induced velocities at the surface are inversely proportional to distance between the vortex element and the point in question on the airfoil.* So, if the strengths and locations of previously shed wake vorticity are known, the instantaneous bound vorticity distribution can be established by enforcing the surface boundary condition (using the known airfoil shape, its motion, and its orientation with respect to the free-stream).

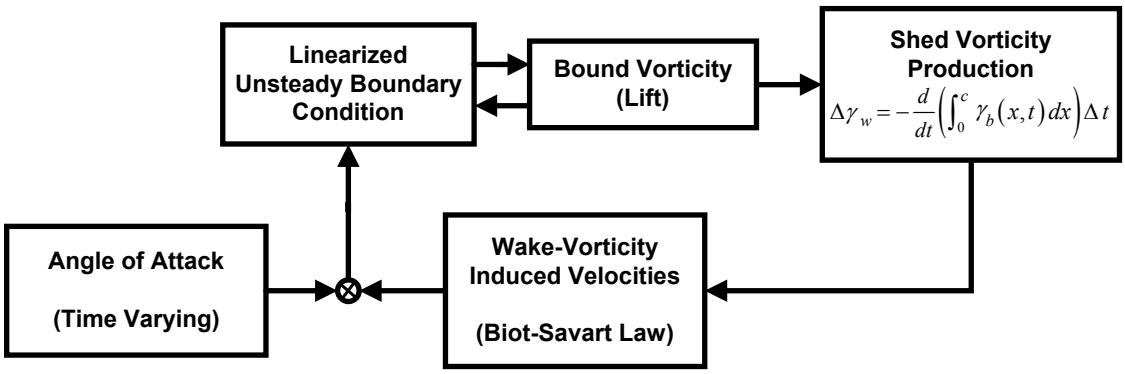

Figure 2-3 Lift, Bound and Wake Vorticity Relationships

Significantly, the lift response involves **two time scales**. The first is a characteristic time for the motion since, in an incompressible fluid, the bound vorticity must respond instantaneously to changes in the airfoil's motion. The second is related to the convection speed of the wake and is due to the residual effects of shed vorticity (which will linger in the vicinity of the airfoil for a time, even if the motion is arrested).

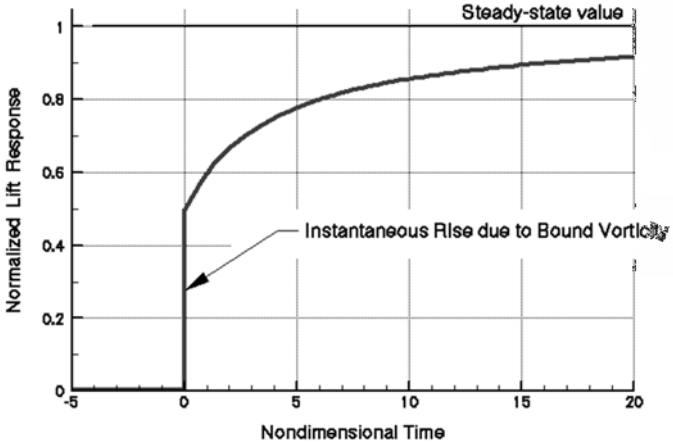

Figure 2-4 - Wagner's function

Consider now an uncambered airfoil, impulsively accelerated from rest to a speed of U_∞ (at a small angle of attack, α). The lift-response time-history, normalized by its steady-state value, (Wagner's function) is shown in Figure 2-4. At the initiation of the motion, the airfoil's bound vorticity must immediately rise to its steady-state value (corresponding to the geometric angle of

* In three dimensional flows, the induced velocities are inversely proportional to the square of the distance.

attack, α). However, this sudden change in bound vorticity must be instantly balanced by vorticity shed into the wake at the trailing edge. The effect of this newly created wake vorticity is to reduce the "effective" angle of attack to one-half its geometric value (due to the wake-induced "cambering" of the airfoil). Subsequently, the shed vorticity propagates downstream and its effect on the induced camber declines. All the while, the bound vorticity responds to the changing effective camber, shedding new vorticity as needed to keep the net vorticity in balance. Ultimately the newly shed vorticity will decrease in strength and travel far enough downstream to have a negligible effect*.

Note that this is identical to the situation where the airfoil has been in motion for a long time (at a fixed angle of attack) but is given a step change in angle of attack (at $t = 0$). Initially the starting vortex is infinitely far downstream and has no effect. After the airfoil is given the instantaneous change in angle of attack, the scenario plays out as described above.

Experience has shown that aerodynamic reactions to small inputs are linear and quite fast-reacting over a large portion of the flight envelope. Indeed, the widely acknowledged success of the stability derivative model is all the evidence needed to support this claim. However, there are phenomena, such as vortex breakdown, that elicit responses that react much more slowly and that are at odds with fundamental assumptions inherent in conventional aerodynamic reaction models. These nonlinear phenomena are the subject of on-going research and are generally beyond the scope of this treatise. However, procedures that can identify the presence of such nonlinearities and that ***should be routinely employed*** will be discussed.

2.4.1 Linear Indicial Responses

The ***linear indicial response*** is a system's response to a unit step input and is of great practical importance.

Summing the lift time histories of all steps inputs occurring in a given time interval provides the net response to an arbitrary motion input. The integral that results in the limit (as the time increment becomes infinitesimal) is called the convolution (or Duhamel's) integral.[6]

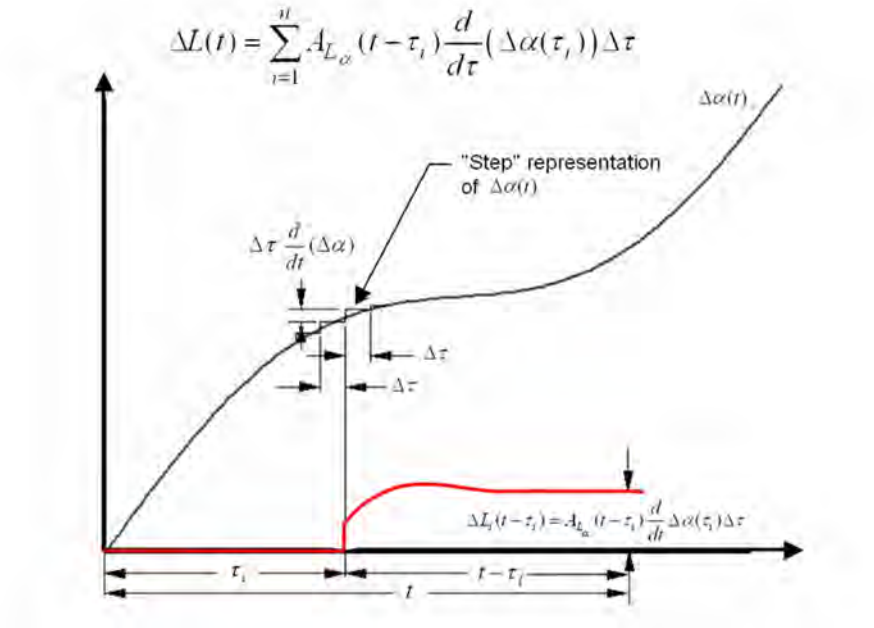

Figure 2-5 -- Superposition Integral

* A mathematician can argue that this requires an infinite length of time, implying that the entire motion history (from the time that the aircraft is rolled out of the hanger) must be known. In practical terms, this is a slight exaggeration. However, the length of time required for wake effects to become negligible is a real issue that we will need to address.

By definition, the lift response to a **unit step** increase in angle of attack at $t = \tau_i$ is denoted by $A_{L_\alpha}(t - \tau_i)$. As shown by the red curve in Figure 2-5, an input at $t = \tau_i$ results in an incremental lift response given by the unit step response scaled by the input step height, $\Delta\tau \frac{d}{dt}\left(\Delta\alpha(t)\right)$. It is necessarily zero for all times prior to $t = \tau_i$ but will affect the net response at all subsequent times.

Thus passing to the limit, the superposition integral becomes.

$$\Delta L(t) = \int_0^t A_{L_\alpha}(t-\tau)\frac{d}{d\tau}\left(\Delta\alpha(\tau)\right)d\tau \qquad \textbf{2-2}$$

Significantly, the indicial response is an ***explicit*** function of time (because we need the influence of all previous inputs to get the net response), while Bryan's stability derivatives are not. It is important to realize that ***both*** the scaling of the indicial responses ***and*** the superposition of the individual step responses (to construct the total response) are made possible by the assumed linearity of the aerodynamic system. In the limit as $\Delta\tau \to 0$, superposition is exact (provided that the indicial response of the system is known precisely).

2.4.2 The "acceleration" Stability Derivatives - Are they really derivatives?

The Dilemma

Experience has shown that the acceleration derivatives are needed. However, since there is no theoretical justification for getting them by expanding the motion variables in a Taylor series, what are the alternatives? The approach taken here is to look for a mathematically sound approximation to the superposition integral. Recalling that ***the superposition integral is exact for a linear system***, we get (as a bonus) a better understanding from a physical standpoint what these terms represent.

So, in lieu of the traditional Taylor series expansion of the motion history function approximating the convolution integral with an ***asymptotic expansion*.**

Asymptotic Expansion – Definition

An asymptotic expansion is an infinite series of functions. It provides an approximation that is increasingly accurate ***as the argument (of the function) approaches a particular value*** known as the limit point, ***L_{pt}***). This is written as

$$f(x) \sim \sum_{n=0}^{\infty} a_n \varphi_n(x) \qquad \left(x \to L_{pt}\right) \qquad \textbf{2-3}$$

where

$f(x)$ is the given function

$\varphi_n(x)$ is a sequence of continuous functions

a_n is the coefficient of the n^{th} term of the sequence

The expansion has some useful properties. Specifically, the error becomes arbitrarily small as the argument **(x)** approaches the limit point, ***regardless of the number of terms* (*N*) *retained in the series***.

Furthermore, the error is bounded by the first ***omitted*** term provided that ***x*** is close enough to ***L_{pt}***.

Approximating the Superposition Integral

The convolution integral, Equation 2-2, written in non-dimensional form is

$$\Delta C_L(\hat{t}) = \int_0^{\hat{t}} A\left(\hat{t}-\tau\right)\frac{d}{d\tau}\left(\Delta\alpha(\tau)\right)d\tau$$

where the "circumflex" denotes a non-dimensional quantity.

Motivated by the success of Bryan's approach, the response as the motion rate approaches zero is sought (because of his assumption that the airloads are a function of the ***instantaneous values*** of the motion variables). Furthermore, the non-dimensional formulation is used because the motion rate relative to the flow's convection speed is the appropriate similarity

parameter. That is, we seek an asymptotic expansion valid as $\frac{\dot{\alpha}\bar{c}}{2U_\infty}$ approaches zero. To this end, expressing the system's response in terms of the difference between its transient and steady-state responses proves useful.

The ***deficiency function***, $F(\hat{t})$, is defined as the difference between the steady-state (long-term) response of the indicial response and its instantaneous value (as shown in Figure 2-6).

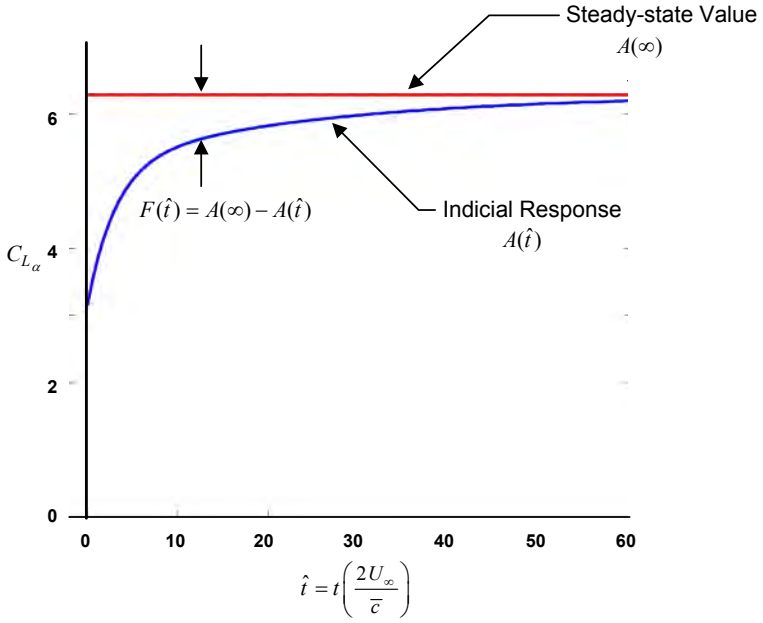

Figure 2-6 - The Deficiency Function

That is

$$\begin{aligned} F(\hat{t}) &= A(\infty) - A(\hat{t}) \\ &= C_{L_\alpha} - A(\hat{t}) \end{aligned}$$

Putting the convolution integral in terms of the deficiency function

$$\begin{aligned} \Delta C_L(\hat{t}) &= C_{L_\alpha}\int_0^{\hat{t}} \frac{d}{d\tau}\Delta\alpha(\tau)\,d\tau - \int_0^{\hat{t}} F(\hat{t}-\tau)\frac{d}{d\tau}\Delta\alpha(\tau)\,d\tau \\ &= C_{L_\alpha}\Delta\alpha(\hat{t}) - \int_0^{\hat{t}} F(\hat{t}-\tau)\frac{d}{d\tau}\Delta\alpha(\tau)\,d\tau \end{aligned}$$

Note that the first term of this form of the superposition integral is simply the long-term response to a unit step input (static lift-curve slope) multiplied by the instantaneous incremental change in angle of attack, i.e., it is identical to Bryan's original formulation. Recasting the integral term by introducing a new dummy variable of integration $\tau_1 = t - \tau$ is instructive**.**

$$\int_0^{\hat{t}} F(t-\tau)\frac{d}{d\tau}\Delta\alpha(\tau)\,d\tau = \int_0^{\hat{t}} F(\tau_1)\frac{d}{d\tau_1}\left(\Delta\alpha(t-\tau_1)\right)d\tau_1$$

But τ_1 is again just a dummy variable so the subscript can be dropped and the superposition integral can also be written

$$\Delta C_L(\hat{t}) = C_{L_\alpha}\,\Delta\alpha(\hat{t}) - \int_0^{\hat{t}} F(\tau)\frac{d}{d\tau}\left(\Delta\alpha(\hat{t}-\tau)\right)d\tau$$

Now, the motion variable (and its time derivatives) can be taken out of the integrand by a successive integration by parts

$$\Delta C_L(\hat{t}) \approx \Delta\alpha(\hat{t})\;C_{L_\alpha} - \Delta\dot{\alpha}(\hat{t})\int_0^{\hat{t}} F(\hat{t})\,d\tau + \Delta\ddot{\alpha}(\hat{t})\int_0^{\hat{t}}\left(\int F(\hat{t})d\tau\right)d\tau - \cdots \qquad \textbf{2-4}$$

Often when approximating an integral, a successive integration by parts does in fact yield an asymptotic expansion. The outcome needs to be verified, however. This can be shown to be true provided that that the ***motion is slow compared to the aerodynamic reaction***. The latter condition implies that the deficiency function becomes negligible much faster than changes in angle of attack (and its time-derivatives) can accumulate. That is over the ***short*** non-dimensional time interval where $F(\hat{t})$ is ***not negligible*** $\Delta\alpha(\hat{t}-\tau) \approx \Delta\alpha(\hat{t})$.

Comparing Equation 2-4 to the general asymptotic representation (Equation 2-3)

$$\frac{d^n}{dt^n}\left(\alpha(\hat{t})\right) \to \varphi_n(x) \qquad \text{and} \qquad \int_0^t \int^{(n-1)} F(\tau)\, d\tau^n \to a_n$$

Finally, the integrals can be related to particular "stability derivatives", e.g., consider a Taylor series expansion of the form:

$$C_L = C_{L_\alpha}\alpha + C_{L_{\dot{\alpha}}}\frac{\dot{\alpha}U_\infty}{2\bar{c}} + C_{L_{\ddot{\alpha}}}\frac{\ddot{\alpha}{U_\infty}^2}{(2\bar{c})^2} + \cdots \qquad \textbf{2-5}$$

Equating terms linear in alpha-dot from this expression and from the asymptotic expansion, Equation 2-3, we have:

$$C_{L_{\dot{\alpha}}} \equiv -\int_0^{\hat{t}} F(\tau)\, d\tau$$

That is, the negative of the area under the deficiency-function curve is ***equivalent*** to the stability derivative relating ***lift to the rate-of-change of angle of attack***. Likewise, the second integral of the deficiency function can be related to the lift due to alpha-double-dot derivative, i.e.

$$C_{L_{\ddot{\alpha}}} \equiv \int_0^{\hat{t}} \left(\int F(\tau)\, d\tau \right) d\tau$$

Note that these "stability derivatives" are not derivatives at all. They are the coefficients of an asymptotic expansion for the convolution integral and are needed to account for the lag in the aerodynamic response to an infinitesimal step input. If the expansion (Equation 2-3) can be truncated after the second term, the transient time for the lag to build up is negligibly small, i.e. the ***approximation*** to the response is not an explicit function of time.

The range of applicability as given by the two derivations (a Taylor series expansion vs. an asymptotic expansion) is quite different, ***even though the resulting equations have the same form***, i.e., they both lead to a series linear in the motion variable and its time derivatives. Applicability, from the asymptotic expansion point of view, simply requires that the $(n+1)^{\text{th}}$ derivative of the non-dimensional motion variable be small (for all n retained in the expansion; i.e. $n \le N$). This is always possible, provided that the motion is slow enough. On the other hand, convergence of Equation 2-5 requires that the ***ratio*** of the $(n+1)^{\text{th}}$ and n^{th} ***terms*** of the expansion goes to zero in the limit ***as n goes to infinity***. Convergence is not an issue with the asymptotic expansion since it is accurate in the limit as the motion-rate parameter approaches zero (***regardless of the number of terms retained in the expansion***). Accuracy is the only issue: the error is on the order of the first omitted term. "Dynamic stability derivatives" can be justified only on the basis of an asymptotic expansion of the convolution integral.

Although they are not actually derivatives, we will continue to call these coefficients stability derivatives (in deference to their historical origin) even though this is a misnomer. This may appear to be hypercritical of the standard terminology. However, we will see that the insight gained can be useful in laying out an experimental program and interpreting the results.

But first, a quick review of some nomenclature is in order. Stability derivatives are broadly divided into two main groups, longitudinal and lateral/directional. Longitudinal derivatives are those associated with forces and moments acting in the vehicle's plane of symmetry due to motions also lying in the plane of symmetry, i.e., translational velocities along and normal to the vehicle centerline and "pitching" motions (angular motions about an axis normal to the plane of symmetry). Lateral/directional derivatives relate forces, moments and motions in two planes normal to each other and to the plane of symmetry. There can also be "cross" derivatives which relate longitudinal forces/moments to lateral/directional motions and vice-versa.

These groups are subdivided into "static" and "dynamic" derivatives. By convention, static stability derivatives are those associated with the forces and moments caused by a vehicle translational velocity perturbation (relative to a reference flight condition) or equivalently by a change in the angular orientation of the vehicle relative to the free-stream velocity vector**.**

On the other hand, dynamic derivatives are those that relate changes in the forces and moments to the vehicle's translational acceleration or angular velocity. Often, these are referred to as the "damping" derivatives. Note that the angular rate derivatives are "dynamic" only in a limited sense. As suggested above, even though angular ***velocities*** are involved they can be associated with a steady-state flow field.

What if the aerodynamic response is not so fast?

The following data, taken from AIAA-2004-5273,[7] illustrates a common problem at high angles of attack. Roll damping characteristics of the fighter aircraft configuration shown in Figure 2-7 were examined over a large range of angle of attack and roll rates. Harmonic roll motions in the NASA Langley 14x22 Foot Subsonic Wind Tunnel were used to determine its roll-damping characteristics.

Figure 2-7 - Fighter Model in Langley 14' x 22' Tunnel

The conventional roll-damping derivative, C_{l_p} was calculated from these data, as shown in Figure 2-8.

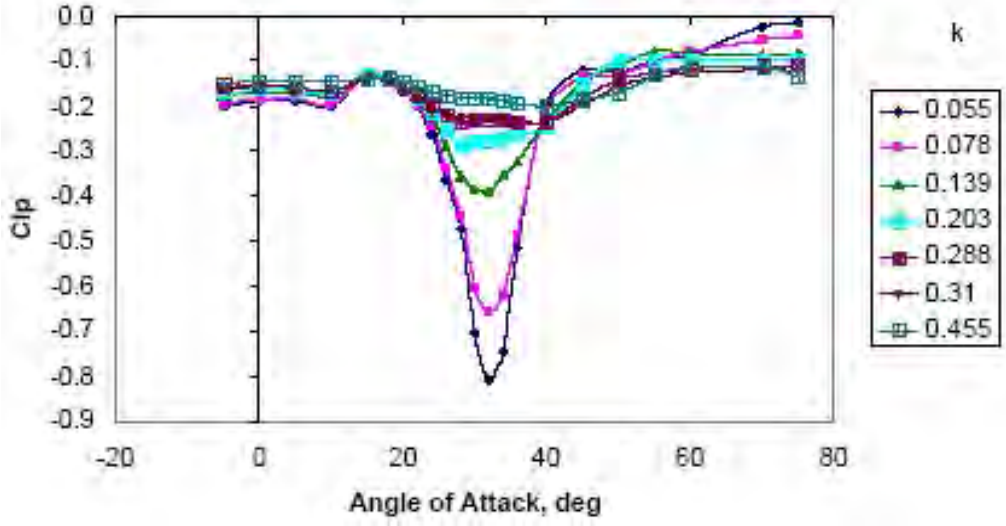

Figure 2-8 - Conventional Roll-Damping Derivative vs. Angle of Attack

The problem is that, from a given steady-state flight condition, the damping derivative is not unique: it is highly dependent on the reduced frequency, especially in the 20 to 40 degree angle of attack range. This is unacceptable because ***harmonic motion frequency*** does not apply to arbitrary motions; the stability derivative concept is clearly not up to the task.

If the both the static and dynamic rolling moment derivatives are linear and time-invariant, the plot of rolling moment vs. the instantaneous roll angle will be an ellipse as shown in Figure 2-9.

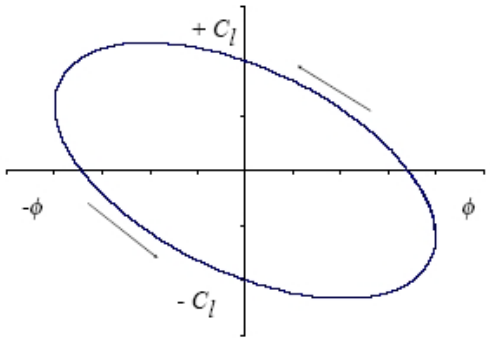

Figure 2-9 - Linear Static and Dynamic Aerodynamics for Harmonic Motions

Wind tunnel data for three reduced frequencies are shown in Figure 2-10. The roll rates and amplitudes were chosen such that the maximum roll rate (as the model passes through zero roll angle) are the same for each motion. Therefore, if a stability derivative model (retaining two terms in the expansion) is valid, all traces will collapse to the same point at $\phi = 0$ because the instantaneous values for both ϕ and $\dot{\phi}$ are identical.

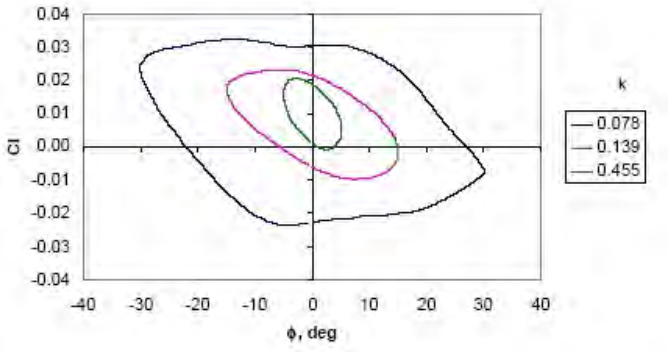

Figure 2-10 - Fighter Configuration Static and Dynamic Aerodynamics, 30 deg. AOA

This is clearly ***not the case*** here. It is interesting to note that as the frequency increases the response shape approaches the classic elliptical shape. This is likely due to the fact that the dynamic aerodynamic response is operating on two time scales. The slower of these simply cannot respond to the high frequency input.

Note also, at the maxima (minima) of the roll angle excursions where the instantaneous roll rates are zero, the rolling moment should (according to the stability derivative model) correspond to the static test values at those roll angles. However, a curve drawn through these points in Figure 2-10 has a considerable rolling moment offset at high frequencies and small roll angles. This is reminiscent of Wagner's function whose instantaneous rise (due to the fast reacting bound vorticity component) is the only part of the response that can follow the high frequency input. Furthermore, there is no reason to expect that these values will be anywhere near the static response. The message is that ***even the use of static derivatives is called into question for rapid motions.*** This knowledge provides a useful diagnostic tool when performing dynamic testing in the tunnel.

2.4.3 Aerodynamic Transfer Functions

Suppose that a vehicle motion (not necessarily periodic) starts from a steady-state condition at $t = 0$. The motion is represented by a perturbation in angle of attack, $\Delta\alpha = \alpha(t) - \alpha_0$. In this case, the resulting lift time history can be expressed in terms of the lift perturbation from its initial steady-state value, L_0.

$$\Delta L(t) = L(t) - L_0 = \Delta L\left(\alpha_0, \Delta\alpha(t), t\right)$$

Following conventional practice, the motion is now limited to ***small perturbations*** from the steady-state equilibrium condition. Under these conditions, the aerodynamic response to a given motion input may ***usually*** be linearized and the "aerodynamic system" taken as stationary, i.e., ***the response is governed by a linear ODE with constant coefficients***. The perturbation in lift has a zero initial value because it represents the deviation from the constant equilibrium condition, L_0.

For example, consider the system governed by the following differential equation and its associated initial conditions:

$$\frac{d^2}{dt^2}x(t) + a\frac{d}{dt}x(t) + b\,x(t) = \alpha(t)$$

$$x(0) = x_0, \qquad \frac{d}{dt}x(0) = \dot{x}_0$$

where: a and b are constants

$\alpha(t)$ is the forcing function (input)

Noting that the Laplace transforms of the derivatives are

$$\mathcal{L}\left(\frac{d^2}{dt^2}x(t)\right) = s^2\bar{x} - s\,x_0 - \dot{x}_0$$

$$\mathcal{L}\left(\frac{d}{dt}x(t)\right) = s\,\bar{x} - x_0$$

where the "over-bar" denotes the Laplace transform of the independent variable

the transfer function for the system is

$$G(s) = \frac{\bar{x}(s)}{\bar{\alpha}(s)} = \frac{\dot{x}_0 + (s+a)x_0 + \bar{\alpha}(s)}{\left(s^2 + a\,s + b\right)\bar{\alpha}(s)}$$

A linear and stationary system's transfer function depends on both its initial conditions and the motion. Transfer function parameters depend only on the initial conditions and remain constant throughout the ensuing motion. Furthermore, if $x(t)$ is a perturbation from an equilibrium condition, i.e., the system is initially at rest and $x(0) = 0$, the transfer function is independent of the input, i.e.

$$G(s) = \frac{\bar{x}(s)}{\bar{\alpha}(s)} = \frac{1}{\left(s^2 + a\,s + b\right)}$$

This is a perfectly general result, so the motion-history function need not be replaced by a Taylor series expansion. If the transfer function is known for a characteristic input, the perturbation in lift for ***any other*** input, $\Delta\alpha(t)$, can be found by taking the inverse Laplace transform of

$$\overline{\Delta L}(s) = \overline{G_{L_\alpha}}(s)\;\overline{\Delta\alpha}(s) \qquad \textbf{2-6}$$

An ***aerodynamic transfer function***, so defined, is an idea first proposed by Etkin[8].

Note that the inverse transform of Equation 2-6 replicates, in the time domain, both the transient and steady-state responses of the linear system because it represents the ***complete*** solution of the governing differential equation.

The transfer function is the aerodynamic system's response to a unit impulse (the Laplace transform of the unit impulse function is equal to "1"). ***Since the Fourier representation for the impulse function requires contributions from all frequencies, the experimental determination of aerodynamic transfer functions is problematic.*** Furthermore, the mathematical form of the transform must be assumed a priori (direct measurements of its parameters are not possible in the time domain).

2.4.4 Frequency Response

Steady-state responses to harmonic forcing (i.e., the response after all transients have died out) can be represented by a complex number called the ***frequency response function*** [9]. It is composed of the product of the ***static gain*** (the amplitude of the ***quasi-steady*** response) and the ***dynamic gain*** (the steady-state harmonic response normalized by the static gain). When plotted in the complex plane, the dynamic gain is a vector whose length gives the amplitude of the response as a percentage of the quasi-steady amplitude. The angle between the real axis and the vector corresponds to the phase angle, ϕ, between the forcing function (motion) and the output (aerodynamic force/moment). Negative values of ϕ correspond to a lag in the response. Frequency response functions can be derived from the system transfer function by replacing "s" with "ik" (where $i = \sqrt{-1}$), dividing by the static gain, and finding the real and imaginary parts of the result. Conversely if the frequency response is known, the transfer function can be determined by replacing "k" with "$-is$" and multiplying by the static gain.

2.4.5 Summary of Linear Response Models

The response models considered thus far have the following restrictions imposed on them: **(1)** the motion is initiated from a ***steady equilibrium condition***, **(2)** the models express the response to ***small perturbations*** from the initial condition (which implies that there are no inputs at $t = 0^-$), and **(3)** the perturbations in lift are governed by ***linear differential equations with constant coefficients***. The last restriction ensures that the corresponding transfer functions, indicial responses, and frequency response functions depend only on the initial equilibrium (steady) flight condition, i.e., they are unique and cannot change in response to the ensuing motion. Subject to these restrictions, the following observations are made:

(1) Frequency response functions represent the steady-state responses to harmonic forcing. They are ***not*** valid aerodynamic models for use in flight mechanics analyses since they are not applicable to arbitrary motion inputs and do not include transient responses. However, many model identification techniques (to determine model parameters from experimental and/or computational data) are based on their mathematical properties. If data are available over a wide range of input frequencies, other model forms (namely aerodynamic transfer functions, indicial responses, and stability derivatives) can be easily computed.

(2) Both the ***indicial response*** and the ***aerodynamic transfer function*** represent ***complete*** solutions to the governing linear differential equation and therefore include transient responses due to an impulsive motion onset from the initial steady-state flight condition. Transients following an abrupt cessation of the motion can also be included by properly defining the input motion.

(3) Note that the Taylor series expansion of the input motion is not required for these models. Motion history effects appear in two ways. First, the transfer function, the indicial response and therefore the stability derivative models depend on the initial flight condition (which implies that the flow field has reached a steady-state condition i.e., the prior motion has been fixed at that condition for a "long" time). Second, the motion history determines the distribution of vorticity in the wake. Motion history always resides in the wake.

(4) Linear models (excepting stability derivatives) ***can*** account for ***multiple time scales and transient effects***. Stability derivatives are valid only for slow motions and being time-invariant ***cannot*** handle transients of any sort.

(5) ***Static stability derivatives*** can be properly considered as the coefficients of a Taylor series expansion of the aerodynamic force/moment in terms of the motion variable (angle of attack; sideslip angle; ***steady*** roll, pitch or yaw rates, or control surface deflection) since each of these can be evaluated from a steady flow condition. Regardless of motion rates, they represent the long term response to a steady input.

(6) ***Dynamic stability "derivatives"***, sometimes called the ***acceleration*** derivatives, are correctly interpreted as the coefficients of an asymptotic expansion of the convolution integral (the "summation" . As such their applicability is restricted to slowly (compared to the aerodynamic response) changing motions. Achievable accuracy with a stability derivative model is influenced by the nature of the motion as well as its speed.

(7) Although the two-dimensional airfoil was used as an example throughout this section, its response is sufficiently fast that these particular effects are seldom important for rigid body flight mechanics analyses at low angles of attack. However, that being said, the need to model "downwash lag" (for wing-on-tail aerodynamic interference

effects) has long been recognized. Furthermore, other sources for much slower reacting aerodynamic forces (notably vortex breakdown) exist at higher angles of attack. These can be so slow that acceptable accuracy with a stability derivative based model is out of the question.

2.5 Coordinate Systems for Flight Mechanics Analysis

Flight vehicle dynamics differ from most other problems in dynamics because the aerodynamic forces/moments and the motion are coupled. Obviously, the vehicle motion needs to be described relative to a coordinate system that simplifies (or rather, does not overly complicate) the expression of these motion dependent forces. However, what is best for an aerodynamic representation may complicate other terms in the equations of motion. (Vehicle moments and products of inertia are time varying in an axis system that is not "fixed" to the aircraft). Furthermore, the chosen coordinate system should also be compatible with experimental techniques necessary to determine configuration specific aerodynamic parameters (see Figure 2-1).

Describing the vehicle's translational and rotational velocity ***relative to the air mass*** is essential (because this is the ***only*** motion relevant to the aerodynamic forces). Also, the orientation of these vectors in relation to the vehicle's external shape is crucial. Therefore, more than one coordinate system is usually involved (in addition to the inertial reference frame). One of these must always be a body-fixed system (needed to locate configuration geometry). Of course this means that we must be careful to specify which coordinate system is being used to define each vector quantity. We must also be able to transform from one system to another at will.

2.5.1 Flight Mechanics Conventions

Virtually all useful coordinate systems require that the origin of the axis system be "attached" to a specified point in/on the vehicle, usually its center of gravity. The linear velocity vector of the axis system's origin relative to the air mass is expressed in terms of its three components relative to the body-fixed system. An alternative is to specify the magnitude of the translational velocity vector ***and*** two angles (between the velocity vector and selected body-axes, angle of attack and side-slip angle, e.g.). Angular velocity components (about each of the body-fixed axes) are used to describe the rotational motion relative to the air mass. However, there are many possible options regarding the orientation of the axes.

Any two of these axis systems can be made coincident by three successive rotations about the ***x***, ***y***, and ***z*** axes of either one.[10] Knowledge of these "Euler" angles provides the means for relating linear and angular velocity vectors expressed in any other system to the body-fixed axes. When transforming from a general axis system to the body-fixed system Euler angle rotations are always yaw, pitch, and finally roll in that order; i.e., a rotation about the ***z*** axis, followed by a rotation about the new ***y*** axis, and finally a rotation about the final ***x*** axis.

Wind (or Air Path) Axes

"Wind axes", have the "$\boldsymbol{x_a}$" axis ***always*** aligned with the vehicle's instantaneous velocity vector; i.e., in the "free-stream" direction. They also ***roll*** with the aircraft (the "$\boldsymbol{z_a}$" axis always lying in its plane of symmetry, i.e., the $\boldsymbol{z_b}$-$\boldsymbol{x_b}$ reference plane), as shown in Figure 2-11. Two "aerodynamic" angles, α and β, specify the orientation of the velocity vector relative to the body-fixed system. Both α and β are measured ***from*** the projection of the x_a-axis (i.e. $\overrightarrow{U_\infty}$) onto the $\boldsymbol{z_b}$-$\boldsymbol{x_b}$ plane. The ***angle of attack***, α, is the angle between this reference line (the red vector, x_1 in the figure) and the x body axis; whereas β (***sideslip angle***) is the angle to $\overrightarrow{U_\infty}$. Note: α and β are actually the Euler-angle rotations required to make the body-axis and the wind axes coincident: the rotation sequence going from wind axes to body axes is -β, α, 0. That is, starting with the wind axes, the rotation -β about $\boldsymbol{z_a}$ is followed by the rotation α about the "new" location of the y_a axis gets us to the body-axis system.

Components of this reference frame's angular velocity (relative to an inertial reference) are denoted p_w, q_w, and r_w about the x_a, y_a, and z_a axes respectively. Note: we will drop the subscripts when no ambiguity results.

The components of ***any vector*** (linear or angular velocity, force or moment) expressed in wind axes are related to its components along the body-axes through:

$$\begin{pmatrix} v_x \\ v_y \\ v_z \end{pmatrix} = \begin{pmatrix} \cos(\alpha)\cos(\beta) & -\cos(\alpha)\sin(\beta) & -\sin(\alpha) \\ \sin(\beta) & \cos(\beta) & 0 \\ \sin(\alpha)\cos(\beta) & -\sin(\alpha)\sin(\beta) & \cos(\alpha) \end{pmatrix} \begin{pmatrix} v_{x_a} \\ v_{y_a} \\ v_{z_a} \end{pmatrix} \qquad \textbf{2-7}$$

To convert from body to wind axes, premultiply this equation by the inverse of the transformation matrix. However, the ***Euler angle transformation matrices*** have the special property that their ***transposes and inverses are equal***. Therefore, premultiplying by the transpose of the transformation matrix produces the desired result.

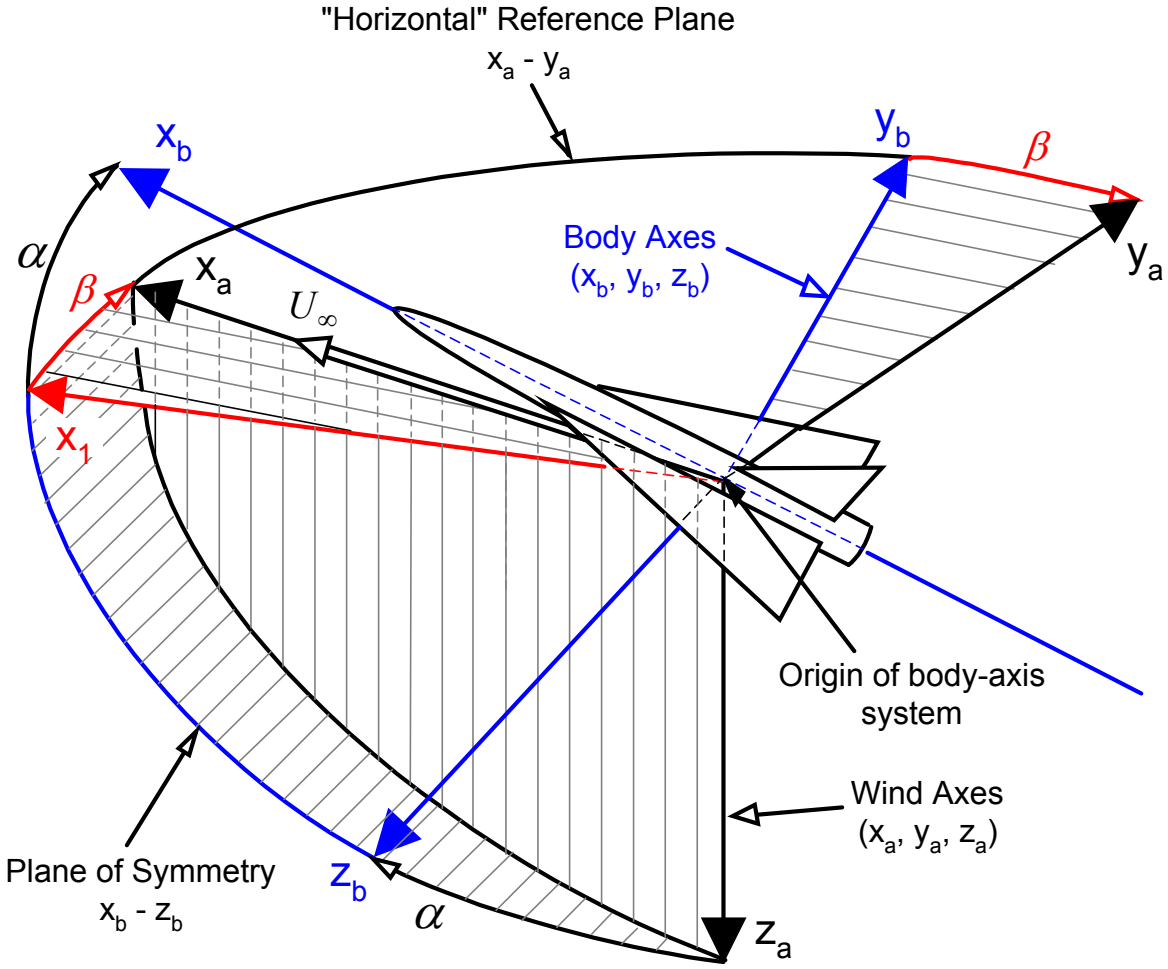

Figure 2-11 - Orientation of the Vehicle With Respect to the Wind- and Body-Axis Systems

Wind axes are particularly convenient for ***static*** tests in the wind tunnel. Since the velocity vector (and therefore the x_a axis) is nominally down the centerline of the tunnel, this is actually a tunnel-fixed system. Note that x_a-y_a plane, labeled the "horizontal" reference plane in the figure, will be horizontal in the tunnel (if the test section itself is horizontal) which aligns the z_a axis with the gravity vector. However, in flight x_a-y_a plane is perpendicular to the aircraft's plane of symmetry and the x wind axis is tangent to the flight path. Note that α and β are all that are needed to specify the orientation of the velocity vector with respect to the vehicle (***bank angle has no effect on the aerodynamic forces***). Thus the only possible difference between wind axes in the tunnel and in flight is the orientation of the x_a-y_a plane (and therefore the z_a axis which is no longer constrained to be vertical). In flight, the vehicle's instantaneous velocity vector can be at any arbitrary orientation with respect to the earth. Similarly, there are no restrictions on the orientation of its plane of symmetry.

Aeroballistic Axes

A second system, shown in Figure 2-12 is known as the "total angle-of-attack" (or the aeroballistic) system. It is often used for missile and/or projectile analyses because of the high degree of symmetry typical of these configurations. It also has its x-axis, "x_t", ***always*** aligned with the vehicle's instantaneous velocity vector. Therefore, it too is a tunnel-fixed system. Total angle of attack, α_t, is the angle between the velocity vector and the x body axis. By definition, the reference plane for this system is the z_t-x_t plane. Unlike wind axes, in general its z-axis, z_t, ***does not*** lie in the vehicle's plane of symmetry. Rather, z_t is perpendicular to x_t and lies in the x_b-x_t plane. The right-handed system is completed by $\mathbf{y}_t$. Axes $\mathbf{y}_t$ and $\mathbf{z}_t$ ***do not*** roll with the vehicle. As a consequence, the second angle (aerodynamic roll angle), ϕ', is needed to specify the orientation of the total angle of attack with respect to the body-fixed axes. Going from aeroballistic axes to body axes, the order of rotation is α_t (about the $\mathbf{y}_t$ axis) followed by ϕ' (about the $\mathbf{x}_b$ axis). The red vector, $\mathbf{z}_1$, is the intermediate position of the z axis (after the first rotation).

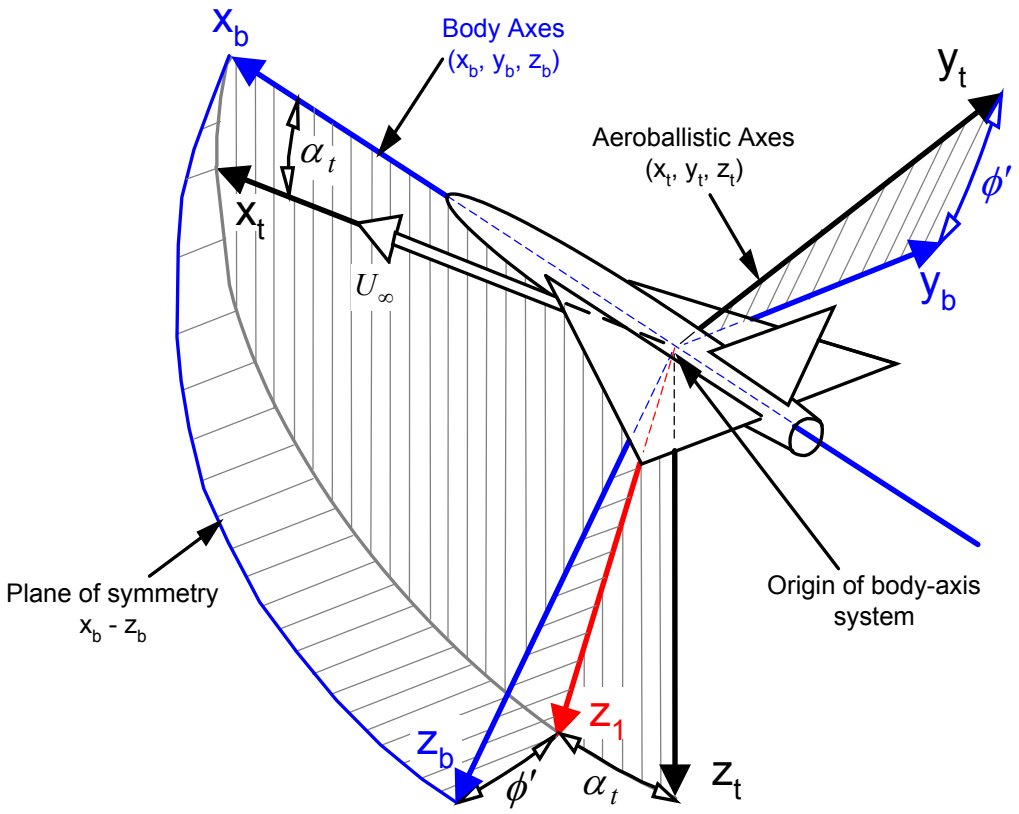

Figure 2-12 Vehicle Orientation in the Aeroballistic System

In the wind tunnel the $\mathbf{x}_t$ axis is directed downstream (along the tunnel centerline) and $\mathbf{z}_t$ is vertical (for facilities whose test sections are horizontal).

Components of its angular velocity vector are denoted p_t, q_t, and r_t about the x_t, y_t, and z_t axes respectively. Note again, we will drop the subscripts when no ambiguity results.

The relationship between components of ***any vector*** expressed in the aeroballistic axes and its components along the body-axes is:

$$\begin{pmatrix} v_x \\ v_y \\ v_z \end{pmatrix} = \begin{pmatrix} \cos(\alpha_t) & 0 & -\sin(\alpha_t) \\ \sin(\alpha_t)\sin(\phi') & \cos(\phi') & \cos(\alpha_t)\sin(\phi') \\ \sin(\alpha_t)\cos(\phi') & -\sin(\phi') & \cos(\alpha_t)\cos(\phi') \end{pmatrix} \begin{pmatrix} v_{x_t} \\ v_{y_t} \\ v_{z_t} \end{pmatrix} \qquad \textbf{2-8}$$

Relationships between Euler angles for the wind and aeroballistic systems are:

$$\tan(\alpha) = \tan(\alpha_t)\cos(\phi')$$
$$\sin(\beta) = \sin(\alpha_t)\sin(\phi')$$

Or going in the reverse direction:

$$\cos(\alpha_t) = \cos(\alpha)\cos(\beta)$$
$$\tan(\phi') = \frac{\tan(\beta)}{\sin(\alpha)}$$

These are especially useful equations for static wind tunnel testing because in many facilities sideslip is obtained by using a "pitch-roll" sequence (thereby keeping the model in the center of the test section). Thus, in order to run a "sweep" in sideslip at constant angle of attack, the equivalent combinations of total angle of attack and aerodynamic roll angle must be known. Other considerations (related to dynamic testing) will be discussed later.

Note also that, ***by definition***, the aeroballistic system is only valid for pitch-roll sequences (similarly, wind axes can involve only yaw-pitch sequences). In some facilities, the VWT for example, yaw-pitch-roll sequences are possible. Relationships for this case can be easily derived using the rotation matrices given in Section 4.5 of reference 3.

Stability Axes

Stability axes are the last of the coordinate systems that we will discuss. ***They are a special case of the body-fixed system and combine features of both the body-fixed axes and the wind axes.*** Their primary usefulness is for small perturbation (from a steady reference flight condition) stability and control analyses.

If the flight condition is symmetric ($\beta = 0$), the orientation of stability axes (relative to the body-fixed axes) are given by the wind axes corresponding to the reference flight condition. However, if the vehicle's velocity vector does not lie in the plane of symmetry (for the reference flight condition), the "x" stability axis is taken as the projection of the velocity vector onto the plane of symmetry. ***They are fixed in this position (relative to the vehicle) throughout the ensuing motion.*** Vectors corresponding to the reference flight condition are constants and are denoted with a subscript "0", α_0 or β_0 e.g. Instantaneous values during the ensuing motion are given by the reference value and a time varying perturbation.

$$\alpha(t) = \alpha_0 + \Delta\alpha(t)$$
$$U(t) = U_0 + u(t)$$

With the usual small disturbance assumptions, the equations-of-motion can be linearized with respect to the reference flight condition.

2.5.2 Transforming a Vector's rate of Change

During an arbitrary motion, the body axes are rotating with respect to either the wind axes or the aeroballistic axes. ***Time derivatives of a vector*** observed simultaneously in systems that rotate relative to each other are ***not*** the same vector. Therefore the transformations given above apply to the instantaneous values of the vectors but not to their rates-of-change. Denoting the transformation matrix "L", the transformation of a vector's rate-of-change (going from reference frame "*a*" to frame "*b*", with frame "*a*" considered to be stationary) is given by (see Etkin[10]):

$$[\mathrm{L}]\{\dot{v}_a\} = \{\dot{v}_b\} + \left[\tilde{\omega}_b\right]\{v_b\}$$

where

$$\left[\tilde{\omega}_b\right] = \begin{pmatrix} 0 & -\omega_{z_b} & \omega_{y_b} \\ \omega_{z_b} & 0 & -\omega_{x_b} \\ -\omega_{y_b} & \omega_{x_b} & 0 \end{pmatrix}$$

ω_{x_b}, ω_{y_b} and ω_{z_b} are the components of reference frame $b's$ angular velocity relative to "a"

$\left[\tilde{\omega}_b\right]\{v_b\}$ is the matrix equivalent of the vector operation, $\vec{\omega} \times \vec{v}_b$

$\{\dot{v}_a\}$ and $\{\dot{v}_b\}$ are the time derivatives of the vector as observed in coordinate systems *a* and *b* respectively.

In addition, the translational and rotational velocities of the selected system relative to an inertial frame are needed to complete the description of the vehicle's motion (again see Etkin[10]).

3 Wind Tunnel Testing Considerations

Recall that the procedure for "identifying" aerodynamic models from wind tunnel measurements is based on "characteristic motions" that are specific to the coordinate system being used. ***We are to change one, and only one, of the state variables at a time***. Dynamic testing in the wind tunnel poses some interesting challenges, however. Not the least of these is the difficulty in generating the needed characteristic motions while avoiding sting/support interference effects, keeping the model near the center of the test section (where the flow is relatively uniform), and of course trying to keep the test equipment as simple as possible. While there is some latitude in choosing appropriate characteristic motions, the ones discussed below are based on "small" amplitude harmonic motions.

To understand the complications introduced by making concessions to the wind tunnel environment, we must first know what the properties of each characteristic motion are in free flight. Given this information, an assessment of any particular tunnel implementation is possible. Therefore, the objective of this section is to define each of the characteristic motions in free fight with an eye on the eventual application to dynamic testing in the wind tunnel. In Section 3.3, we will see what single degree-of-freedom rotational motions in the tunnel (by far the most common procedure) will allow us to measure.

Since it's the motion of the test article that is of primary interest, its velocity vectors (either translational or rotational) are expressed in the body-fixed coordinate system. In general, the relationships among the translational velocity components in the body-axis system and any of the axis systems that "track" the velocity vector relative to the air mass are given by

$$\begin{pmatrix} u_b \\ v_b \\ w_b \end{pmatrix} = \left[L_{aero\,b} \right] \begin{pmatrix} u_{aero} \\ v_{aero} \\ w_{aero} \end{pmatrix} \qquad \textbf{3-1}$$

where

"b" denotes body axes

"aero" denotes a generic axis system with its x-axis aligned with the velocity vector

$[L_{aero\,b}]$ is a generic transformation matrix the relates the velocity vectors of the two systems and is expressed in terms of the "aero" system's Euler angles

In the body-axis system, components of the rotation vector in the x, y, and z directions are given by P, Q, and R respectively. The vehicle's forward speed is usually taken as a constant (the rate-of-change of the aerodynamic coefficients with respect to speed are generally negligible except in the transonic Mach number range where compressibility effects vary rapidly). Therefore, the motion variables are the two "aerodynamic angles" (α and β in wind axes, for example) and P, Q, and R. Again, all but one of these must be held constant for each characteristic motion.

3.1 Characteristic Motions in Wind Axes

The vehicle motion is computed by integrating the vehicle's velocity components expressed in a "trajectory" coordinate system which is fixed in space and aligned with the x_a, y_a, z_a system corresponding to the reference flight condition. It is an inertial reference frame.

Recalling that the x wind-axis is aligned with the vehicle's translational velocity vector, Equation 3-1, specialized to wind axes from Equation 2-7, is

$$\begin{aligned} \begin{pmatrix} u_b \\ v_b \\ w_b \end{pmatrix} &= \begin{pmatrix} \cos(\alpha)\cos(\beta) & -\cos(\alpha)\sin(\beta) & -\sin(\alpha) \\ \sin(\beta) & \cos(\beta) & 0 \\ \sin(\alpha)\cos(\beta) & -\sin(\alpha)\sin(\beta) & \cos(\alpha) \end{pmatrix} \begin{pmatrix} U_\infty \\ 0 \\ 0 \end{pmatrix} \\ &= U_\infty \begin{pmatrix} \cos(\alpha)\cos(\beta) \\ \sin(\beta) \\ \sin(\alpha)\cos(\beta) \end{pmatrix} \end{aligned} \qquad \text{3-2}$$

from which the following relationships are seen to hold:

$$\alpha = \tan^{-1}\left(\frac{w_b}{u_b}\right)$$

$$\beta = \sin^{-1}\left(\frac{v_b}{U_\infty}\right)$$

Each characteristic motion is computed by considering small perturbations relative to a ***steady-state*** reference condition (given by $u_a = U_\infty$, $\alpha = \alpha_0$, $\beta = \beta_0$; P, Q and $R = 0$).

The aerodynamic angle perturbations are defined as

$$\Delta\alpha(t) = \alpha(t) - \alpha_0 = \overline{\Delta\alpha}\sin(\omega t)$$

$$\Delta\beta(t) = \beta(t) - \beta_0 = \overline{\Delta\beta}\sin(\omega t)$$

Rotation-rate perturbations are taken to be

$$P = \overline{p}\cos(\omega t)$$

$$Q = \overline{q}\cos(\omega t)$$

$$R = \overline{r}\cos(\omega t)$$

and represent small-amplitude harmonic rotations of the x_b, y_b and z_b axes respectively. Note that cosine functions were chosen to represent these perturbations. Although the choice is arbitrary, this form simplifies the following discussions.

Vehicle displacements and velocity components are summarized in Table 3-1. The reference flight condition is taken to be horizontal, therefore in the inertial coordinate system the x axis is positive forward, the y axis positive out the right wing, and z is positive down. Note that $u_a = U_\infty$ and $x = U_\infty t$ in every case. For the rotation-rate velocity components, the angles ϕ, θ, and ψ are obtained by integrating the rotation-rate perturbations, i.e.,

$$\phi = \overline{p}\frac{\sin(\omega t)}{\omega}$$

$$\theta = \overline{q}\frac{\sin(\omega t)}{\omega}$$

$$\psi = \overline{r}\frac{\sin(\omega t)}{\omega}$$

Keep in mind that these velocity components are those necessary to hold all state variables constant except the one of interest.

Motion	v_a	w_a	y	z
α	0	$\Delta\alpha\, U_\infty \cos\beta_0$	0	$\overline{\Delta\alpha}\frac{U_\infty \cos(\beta_0)}{\omega}\left(1-\cos(\omega t)\right)$
β	$\Delta\beta\, U_\infty$	0	$\overline{\Delta\beta}\frac{U_\infty}{\omega}\left(1-\cos(\omega t)\right)$	0
p	$-\phi\, U_\infty \sin\alpha_0$	$\phi\, U_\infty \cos\alpha_0 \sin\beta_0$	$-\overline{p}\,\frac{U_\infty}{\omega^2}\sin\alpha_0\left(1-\cos(\omega t)\right)$	$\overline{p}\,\frac{U_\infty}{\omega^2}\cos\alpha_0 \sin\beta_0\left(1-\cos(\omega t)\right)$
q	0	$-\theta\, U_\infty \cos\beta_0$	0	$-\overline{q}\,\frac{U_\infty}{\omega^2}\cos\beta_0\left(1-\cos(\omega t)\right)$
r	$\psi\, U_\infty \cos\alpha_0$	$\psi\, U_\infty \sin\alpha_0 \sin\beta_0$	$\overline{r}\,\frac{U_\infty}{\omega^2}\cos\alpha_0\left(1-\cos(\omega t)\right)$	$\overline{r}\,\frac{U_\infty}{\omega^2}\sin\alpha_0 \sin\beta_0\left(1-\cos(\omega t)\right)$

Table 3-1 Characteristic Motions in Wind Axes

Several important factors are immediately apparent.

1. ***All*** of the characteristic motions ***involve curvilinear flight paths*** (note the time-varying trajectory coordinates). Therefore, wind tunnel simulation of every one of these requires both translational and rotational motion(s) since the free-stream velocity is fixed in direction.

2. For the α (and β) motions, ***the amplitude of the required vertical (lateral) excursions is directly proportional to the free-stream velocity and inversely proportional to the frequency***. Therefore, low reduced frequencies lead to relatively large motion requirements, e.g., the z excursions for the α-motion can be rewritten

$$z(t) = \overline{\Delta\alpha}\left(\frac{\bar{c}}{2k}\right)\cos(\beta_0)\left(1-\cos(\omega\, t)\right)$$

3. The angle-of-attack characteristic motion depends on β_0. However, the sideslip motion is ***independent*** of both α_0 and β_0. This a consequence of the rotation order for the Euler angles relating the body and wind axes, i.e., a yaw rotation (sideslip) followed by the pitch rotation (angle of attack).

4. Two of the characteristic motions, p and r, involve both vertical and horizontal translational motions if the reference flight condition is ***not symmetric*** ($\beta_0 \neq 0$).

5. If ***both*** α_0 and β_0 are zero the p-motion flight path is rectilinear. Lateral translational displacements are proportional to $\sin\alpha_0$, while the vertical component is dependent on $\cos(\alpha_0)\sin(\beta_0)$.

Angle-of-Attack Motion

The flight path for the α motion is shown in Figure 3-1. The reference flight condition* is $U_\infty = 50$ fps, $\alpha_0 = 30$ deg., $\beta_0 = 0$ deg., $\omega = 5$ rad./sec (0.8 Hz.) and $\overline{\Delta\alpha} = 2.5$ deg. Note the expanded vertical scale and that the motion is from right to left. Also shown is the time history of the angle-of-attack perturbation.

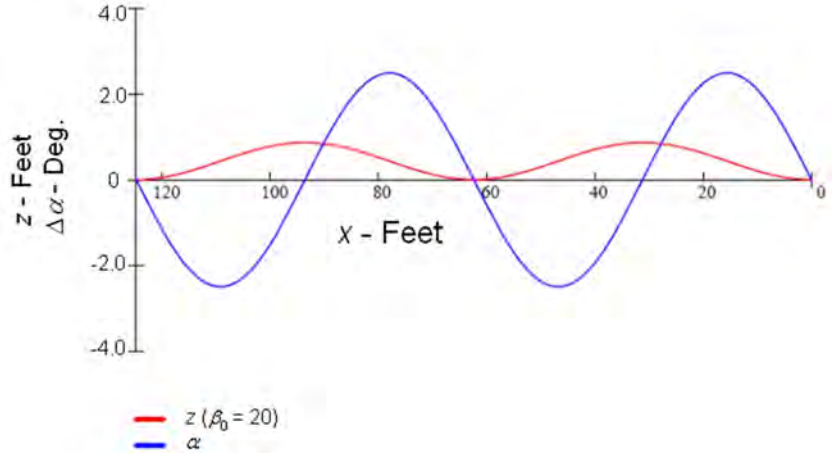

Figure 3-1 - Angle-of-Attack Characteristic Motion

Since rotations are excluded from this particular characteristic motion, angle-of-attack changes have to be generated by a translational motion. Furthermore, the z coordinate is positive downward and a "plunging" ***velocity*** produces a ***positive*** α, i.e.,

$$\alpha = \tan^{-1}\left(\frac{w_b}{u_b}\right)$$

* These are typical of conditions in the VWT at a dynamic pressure of about 3 psf. The longitudinal reduced frequency (i.e. the reduced frequency based on the longitudinal reference length) would be about 0.05 for a reasonably sized model.

Therefore the "z" time history lags the angle of attack by 90° (because $\frac{d\,z}{d\,t} = w_b$). The translational excursion has an amplitude of about 0.4 feet (0.8 peak-to-peak) which is required to generate a 2.5 degree α perturbation. From Equation 3-1, with $\Delta v_b = 0$ to ensure no sideslip motion, u_b must have a harmonic oscillation in order to hold U_∞ constant.

Sideslip Motion

Flight conditions are $U_\infty = 50$ fps, $\omega = 5$ rad./sec (0.8 Hz.) and $\overline{\Delta\beta} = 2.5$ deg. Again, no rotational rates are permitted. Therefore there is nothing new with this motion except that the required translational excursions are in the lateral plane since

$$\beta = \sin^{-1}\left(\frac{v_b}{U_\infty}\right)$$

Again in this case, u_b must be time varying (to hold $\Delta w_b = 0$ and U_∞ constant).

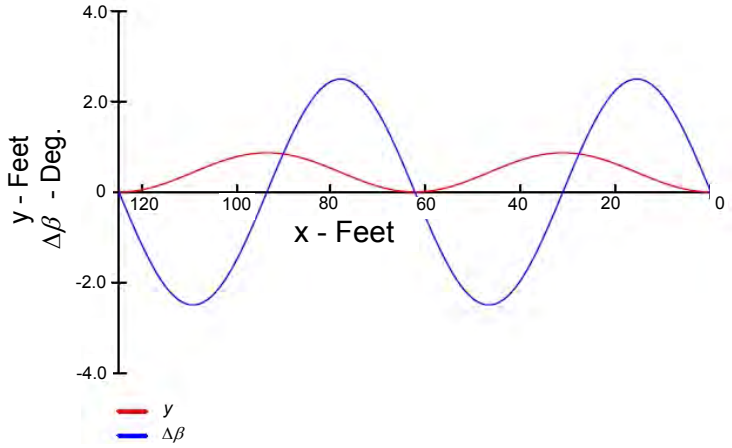

Figure 3-2 - Sideslip Characteristic Motion

3.1.1 Rotation-Rate Characteristic Motions

The significant difference between the rotational-rate characteristic motions and the "aerodynamic angle" motions is that the role of the translational velocities is reversed. In this case, they are required to ***cancel*** (as opposed to generate) the α and β excursions that would be created by the body-axis rotations. For example, when an aircraft in rectilinear flight (at angle of attack and zero sideslip) rolls about its body axis, α is "exchanged" for β. As the roll angle reaches 90° the velocity vector that was lying in the plane of symmetry is now in the lateral plane.

Plots of the rolling, pitching and yawing characteristic motions are presented below. Rotation-rate amplitudes ($\overline{p}$, $\overline{q}$, and $\overline{r}$) are 0.22 rad/sec which corresponds to a peak angular displacement of 2.5 degrees (equal to the amplitude of the α and β motions). Nominal reference flight conditions are $U_\infty = 50$ fps, $\alpha_0 = 30$ deg., $\beta_0 = 20$ deg., and $\omega = 5$ rad./sec.

Rolling Motion

The roll-rate characteristic motion is the "odd man out" case, i.e., **for symmetric flight conditions** ($\beta_0 = 0$), it is the only one whose amplitude varies linearly with α_0 (within the small angle approximation), see Table 3-1. Trajectories for the conditions detailed above are plotted in Figure 3-3. Amplitudes of the remaining rotation-rate characteristic motions are independent of α_0 (under the same assumption) and have close analogs with either the α or the β motions.

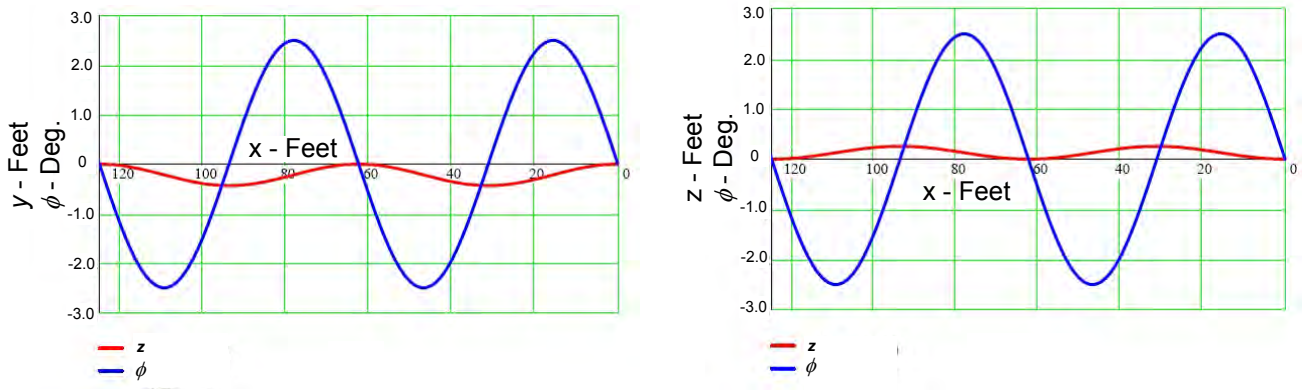

Figure 3-3 -- Rolling Motion Trajectories

Note that the z translational displacement lags the body-axis roll angle ϕ by 90°, while the y time history lags by 270° (or leads by 90°, if you prefer). In other words, the y and z components are 180° out of phase because of the swapping of α for β during body-axis rolls (as mentioned above). When α is at a maximum, β must be at a minimum and vice versa.

Pitching Motion

This case is closely allied with the α motion, the z-coordinates differing only by the factor $-\frac{1}{\omega}$ and the perturbation amplitudes, $\overline{\Delta\alpha}$ and $\overline{q}$. However, if (as was done here) the amplitudes of the ***angular*** excursions in both cases are equal, $\overline{\Delta\alpha} = \frac{\overline{q}}{\omega}$. The minus sign is needed here because the translational velocity must ***cancel*** the α perturbation. As a result, the "z-motion" lags the body-axis pitch angle (θ) by 270°.

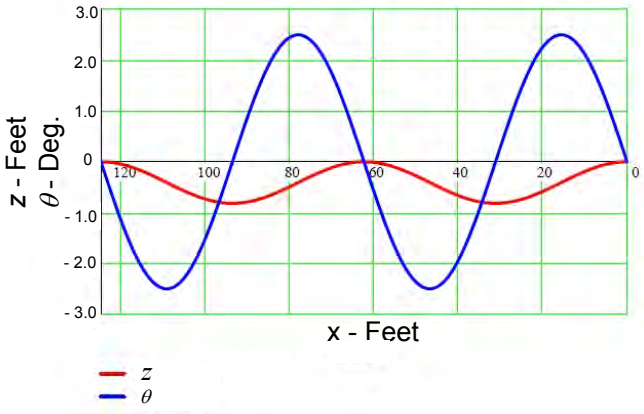

Figure 3-4 -- Pitching Moment Trajectory

Yawing Motion

As expected, the yaw-rate trajectory is closely allied with the β characteristic motion, ***the "y" components*** differing only by the factor $\frac{1}{\omega}\cos(\alpha_0)$ and the perturbation amplitudes, $\overline{\Delta\beta}$ and $\overline{r}$. There is no minus sign here (as opposed to the previous case) because a positive body-axis yaw-angle (ψ) produces a negative β. That is, there are actually two minus signs (one

that would is needed for the lateral translational velocity to cancel the β perturbation and the other to account for the sign difference between ψ and β). Therefore, as in the β-motion case, the "z-motion" lags the "ψ time history" by 90°.

Once more, if the amplitudes of the angular excursions in both cases are equated, $\overline{\Delta\beta} = \frac{\overline{r}}{\omega}\cos(\alpha_0)$. The $\cos(\alpha_0)$ factor comes about because the angle between the z_b and z_a axes is α_0 (see Figure 2-11).

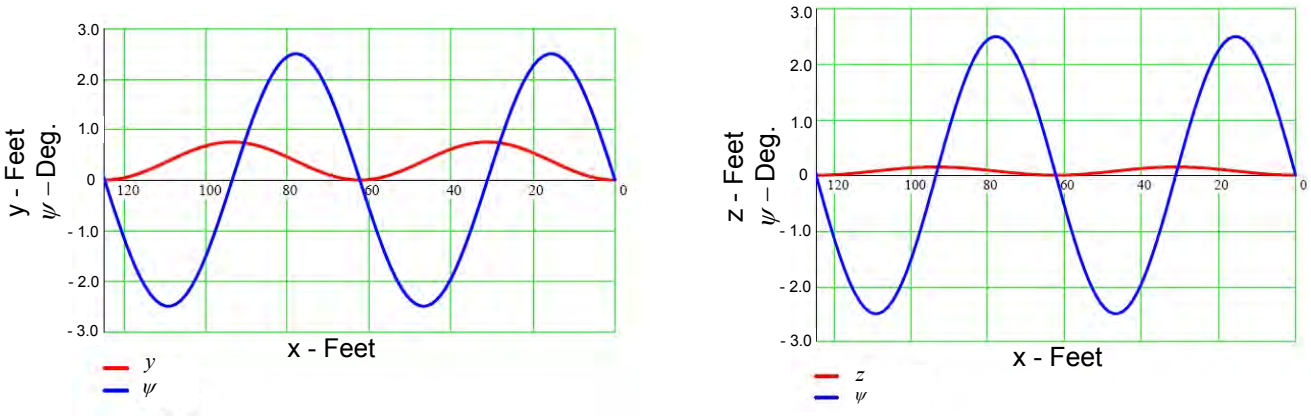

Figure 3-5 -- Yaw Rate Characteristic Motion

Note that there is no *z*-component of the trajectory in symmetric flight. Furthermore, it is a second-order effect if ***both*** α_0 and β_0 are small.

3.2 Characteristic Motions in Aeroballistic Axes

In the aeroballistic axis system, the body-axis velocity components are given, from Equations 2-8 and 3-1, by

$$\begin{pmatrix} u_b \\ v_b \\ w_b \end{pmatrix} = \begin{pmatrix} \cos(\alpha_t) & 0 & -\sin(\alpha_t) \\ \sin(\alpha_t)\sin(\phi') & \cos(\phi') & \cos(\alpha_t)\cos(\phi') \\ \sin(\alpha_t)\cos(\phi') & -\sin(\phi') & \cos(\alpha_t)\cos(\phi') \end{pmatrix} \begin{pmatrix} U_\infty \\ 0 \\ 0 \end{pmatrix}$$

$$= U_\infty \begin{pmatrix} \cos(\alpha_t) \\ \sin(\alpha_t)\sin(\phi') \\ \sin(\alpha_t)\cos(\phi') \end{pmatrix}$$

From which we have

$$\alpha_t = \cos^{-1}\left(\frac{u_b}{U_\infty}\right)$$

$$\phi' = \tan^{-1}\left(\frac{v_b}{w_b}\right)$$

As with the wind-axis system, each characteristic motion is computed by considering small perturbations relative to a ***steady-state*** reference condition (this time given by $u_t = U_\infty$, $\alpha_t = \alpha_{t_0}$, $\phi' = \phi'_0$; P, Q and $R = 0$).

The aerodynamic angle perturbations are defined as

$$\Delta\alpha_t(t) = \alpha_t(t) - \alpha_{t_0} = \overline{\Delta\alpha_t}\sin(\omega t)$$

$$\Delta\phi'(t) = \phi'(t) - \phi'_0 = \overline{\Delta\phi'}\sin(\omega t)$$

Rotation-rate perturbations are taken to be

$$P = \overline{p}\ \cos(\omega\, t)$$
$$Q = \overline{q}\ \cos(\omega\, t)$$
$$R = \overline{r}\ \cos(\omega\, t)$$

and represent small-amplitude harmonic rotations of the x_b, y_b and z_b axes respectively.

Vehicle displacements and velocity components are summarized in Table 3-2. Like before, the reference flight condition is taken to be horizontal and therefore in the inertial coordinate system the x axis is positive forward, the y axis positive out the right wing, and z is positive down. Note that $u_t = U_\infty$ and $x = U_\infty\, t$ in every case. For the rotation-rate velocity components, the angles ϕ, θ, and ψ are obtained by integrating the rotation-rate perturbations, i.e.,

$$\phi = \overline{p}\frac{\sin(\omega\, t)}{\omega}$$
$$\theta = \overline{q}\frac{\sin(\omega\, t)}{\omega}$$
$$\psi = \overline{r}\frac{\sin(\omega\, t)}{\omega}$$

Again, the velocity components given in Table 3-2 are those necessary to hold all state variables constant except the one of interest.

Motion	v_t	w_t	y	z
α_t	0	$\theta\, U_\infty$	0	$\overline{\Delta\alpha_t}\frac{U_\infty}{\omega}\left(1-\cos(\omega t)\right)$
ϕ'	$\Delta\phi'\, U_\infty\, \sin(\alpha_{t_0})$	0	$\overline{\Delta\phi'}\frac{U_\infty}{\omega}\sin(\alpha_{t_0})\left(1-\cos(\omega t)\right)$	0
p	$-\phi\, U_\infty \sin(\alpha_{t_0})$	0	$-\overline{p}\frac{U_\infty}{\omega^2}\sin(\alpha_{t_0})\left(1-\cos(\omega t)\right)$	0
q	$\theta\, U_\infty \sin(\phi')\cos(\alpha_{t_0})$	$-\theta\, U_\infty \cos(\phi')$	$\overline{q}\frac{U_\infty}{\omega^2}\cos(\alpha_{t_0})\sin(\phi')\left(1-\cos(\omega t)\right)$	$-\overline{q}\frac{U_\infty}{\omega^2}\cos(\phi')\left(1-\cos(\omega t)\right)$
r	$\psi\, U_\infty\, \cos(\alpha_{t_0})\cos(\phi')$	$\psi\, U_\infty \sin(\phi')$	$\overline{r}\frac{U_\infty}{\omega^2}\cos(\alpha_{t_0})\cos(\phi')\left(1-\cos(\omega t)\right)$	$\overline{r}\frac{U_\infty}{\omega^2}\sin(\phi')\left(1-\cos(\omega t)\right)$

Table 3-2 Velocity Components and Characteristic Motions in Aeroballistic Axes

The following properties are noted.

1. Again, ***all*** of these characteristic motions ***involve curvilinear flight paths***.
2. Low reduced frequencies require relatively large translational amplitudes for both α_t and ϕ' characteristic motions.
3. Two of the characteristic motions, *q* and *r* this time, involve both vertical and horizontal translational motions if the reference flight condition is ***not symmetric*** ($\phi'_0 \neq 0$).
4. Both of the ϕ' and the *p* characteristic motions are rectilinear if $\alpha_{t_0} = 0$.

3.3 Single Degree of Freedom Motions (Rotation) in the Wind Tunnel

For the reasons discussed in Section 3, wind tunnel dynamic test equipment is generally designed to provide single degree-of-freedom rotational motions. However, as we have seen, these devices cannot produce the motions needed to vary the state variables one at a time. In this section, the effects of single degree-of-freedom motion on the quantities being measured are examined. Effects on measurements in both the wind and aeroballistic axis systems are considered.

3.3.1 Wind (Air-Path) Coordinates

As we have seen, the α and β characteristic motions can be obtained only through translational motions normal to the flight path. These are seldom available in the tunnel. Thus only the rotational motions are considered below.

Pitching Rotations

From Table 3-1**Error! Reference source not found.** for the pitch-rate characteristic motion

$$z_a = -\bar{q}\frac{U_\infty}{\omega^2}\cos\beta_0\left(1-\cos(\omega t)\right) \qquad 3\text{-}3$$

For the α motion we also have

$$z_a = \overline{\Delta\alpha}\frac{U_\infty\cos\beta_0}{\omega}\left(1-\cos(\omega t)\right) \qquad 3\text{-}4$$

Rectilinear motion with a non-zero pitch-rate is thus seen as the superposition of the q and α characteristic motions, i.e., adding Equations 3-3 and 3-4, the z_α perturbation is zero if

$$\overline{\Delta\alpha}\frac{U_\infty\cos\beta_0}{\omega}\left(1-\cos\left(\omega t\right)\right)-\bar{q}\frac{U_\infty\cos\beta_0}{\omega^2}\left(1-\cos\left(\omega t\right)\right)=0$$

or when

$$q=\omega\Delta\alpha$$

Furthermore, since

$$q=\bar{q}\cos\left(\omega t\right)$$

and

$$\theta\left(t\right)=\Delta\alpha\left(t\right)=\overline{\Delta\alpha}\sin\left(\omega t\right)$$

the requirement for rectilinear motion is equivalent to

$$q=\frac{d}{dt}\left(\Delta\alpha\right)$$

In other words, q and $\dot{\alpha}$ ***are numerically equal*** for rectilinear motion and, equally important, ***are in-phase with each other***. This has important implications to dynamic testing and the interpretation of the results. Keep in mind that despite their numerical equality they are distinctly different physical quantities: one represents a translational motion and the other a rotational effect.

Therefore, the pitching rotation in the wind tunnel produces simultaneous changes in α, $\dot{\alpha}$ and q. This issue must be dealt with to properly reduce the data.

Of course, this result is intuitively obvious from the geometry of the wind tunnel. We ***cannot*** (with a single degree-of-freedom rotation device) get a pitch rate without a corresponding effect on angle of attack. However, approaching the problem from the viewpoint of characteristic motions allows us to appreciate the difference between the two effects when applying the results to an arbitrary motion.

Yawing Rotations

Yawing motions are more complicated, especially if both aerodynamic angles (α_0 and β_0) are nonzero. Again, from Table 3-1, the yaw-rate characteristic motion requires translational velocities in the y_a and z_a directions to hold both α_0 and β_0 constant. Therefore, we must look to the characteristic motions for both α and β to find relationships that ensure a rectilinear motion. Thus

$$y_a = \bar{r}\frac{U_\infty}{\omega^2}\cos\alpha_0\left(1-\cos(\omega t)\right)+\overline{\Delta\beta}\frac{U_\infty}{\omega}\left(1-\cos(\omega t)\right)=0$$

and

$$z_a = \bar{r}\frac{U_\infty}{\omega^2}\sin\alpha_0\sin\beta_0\left(1-\cos(\omega t)\right)+\overline{\Delta\alpha}\frac{U_\infty\cos(\beta_0)}{\omega}\left(1-\cos(\omega t)\right)=0$$

Therefore

$$\overline{\Delta\beta} = -\frac{\bar{r}}{\omega}\cos(\alpha_0)$$

$$\overline{\Delta\alpha} = -\frac{\bar{r}}{\omega}\sin(\alpha_0)\tan(\beta_0)$$

Hence a single degree of freedom ***body-axis*** yaw rate induces perturbations in β and α. The relationships for their rates of change are

$$\dot{\beta} = -r\cos(\alpha_0) \text{ and } \dot{\alpha} = -r\sin(\alpha_0)\tan(\beta_0)$$

It is worth noting that the angle-of-attack perturbation is small for small β_0 and vanishes altogether for a symmetric reference flight condition. In general however, the yaw-rate motion involves simultaneous changes in α, $\dot{\alpha}$, β, $\dot{\beta}$ and r. Again the fact that both $\dot{\alpha}$ and $\dot{\beta}$ are in phase with r is noteworthy.

Rolling Rotations

Roll-rate induced effects for rectilinear motion are derived in the same manner. In this case we find the following relationships:

$$\overline{\Delta\alpha} = -\frac{p}{\omega}\cos(\alpha_0)\tan(\beta_0)$$

$$\overline{\Delta\beta} = \frac{p}{\omega}\sin(\alpha_0)$$

$$\dot{\alpha} = -p\cos(\alpha_0)\tan(\beta_0)$$

$$\dot{\beta} = p\sin(\alpha_0)$$

Again, the α perturbations disappear for symmetric flight.

Summary of Wind-Axis Results

There is both good news and bad news regarding single degree-of-freedom rotational motions in the wind tunnel. First, the bad news: although each rotary motion contains the desired effect (p, q, or r characteristic motions), each is "contaminated" by characteristic motions belonging to the "aerodynamic angles" α and/or β. Furthermore, some of this contamination is in phase with the rotation rates. This means that ***if*** the aerodynamic reactions to the motion are instantaneous, as assumed by the stability derivative model, there is no way to isolate the effects of the translational and rotational motions and we must accept a measurement of their combined effects.

Now the good news: we do in fact want to know what the effects of the state variables associated with the translational characteristic motions are. In particular, the effect of their rate of change* is needed, since static tests can provide changes

* Recall that $\dot{\alpha}$ and $\dot{\beta}$ stability "derivatives" are a measure of the lags inherent in an aerodynamic response.

due to the instantaneous values of these motion variables. Therefore, having the combined effect is (in some sense) better than nothing. Provided that an estimate (from a theoretical prediction or from another source) for the other components of the combined measurement is available, an estimate for the individual effects is possible. Amplitudes of the "corrupting" characteristic motions ($\overline{\Delta\alpha}$ and $\overline{\Delta\beta}$) and the relationships between the instantaneous rates-of-change of these motion variables ($\dot{\alpha}$ and $\dot{\beta}$) and the rotational rates for each of the motions are summarized in Table 3-3.

Motion	$\overline{\Delta\alpha}$	$\overline{\Delta\beta}$	$\dot{\alpha}$	$\dot{\beta}$
Roll	$-\frac{\overline{p}}{\omega}\cos(\alpha_0)\tan(\beta_0)$	$\frac{\overline{p}}{\omega}\sin(\alpha_0)$	$-p\cos(\alpha_0)\tan(\beta_0)$	$p\sin(\alpha_0)$
Pitch	$\frac{\overline{q}}{\omega}$	0	q	0
Yaw	$-\frac{\overline{r}}{\omega}\sin(\alpha_0)\tan(\beta_0)$	$-\frac{\overline{r}}{\omega}\cos(\alpha_0)$	$-r\sin(\alpha_0)\tan(\beta_0)$	$-r\cos(\alpha_0)$

Table 3-3 Rectilinear Motion in Wind Axes

3.3.2 Aeroballistic (Total Angle-of-Attack) Axes

The procedure for finding which (and how much of each) characteristic motions can be superimposed to produce a desired rectilinear motion is, of course, independent of the coordinate system. However, the combination for a given motion may not be unique as we will see below. The "contaminating" characteristic motions (that occur when the rotation-rate motions are superimposed with those associated with the aerodynamic angles) are summarized in Table 3-4. The equations used to derive these results are presented in Table 3-2.

Motion	$\overline{\Delta\alpha_t}$	$\overline{\Delta\phi'}$	$\dot{\alpha}_t$	$\dot{\phi}'$
Roll	0	$\frac{\overline{p}}{\omega}$	0	p
Pitch	$\frac{\overline{q}}{\omega}\cos(\phi'_0)$	$-\frac{\overline{q}}{\omega}\cot(\alpha_{t_0})\sin(\phi'_0)$	$q\cos(\phi'_0)$	$-q\cot(\alpha_{t_0})\sin(\phi'_0)$
Yaw	$-\frac{\overline{r}}{\omega}\sin(\phi'_0)$	$-\frac{\overline{r}}{\omega}\cot(\alpha_{t_0})\cos(\phi'_0)$	$-r\sin(\phi'_0)$	$-r\cot(\alpha_{t_0})\cos(\phi'_0)$

Table 3-4 Rectilinear Motion in Aeroballistic Axes

There is an apparent problem concerning the amplitudes of the ϕ' characteristic motions for pitching and yawing motions. At low total angle-of-attack, the contribution of the ϕ' motion (needed to ensure rectilinear motion) becomes very large. The source of the problem can be traced to the results presented in Table 3-2. Both the pitching and yawing characteristic motions require *y*-components of translational velocities proportional to $\cos(\alpha_t)$. However, ϕ' is the only aerodynamic angle motion available to cancel the *y*-velocity component, and it is proportional to $\sin(\alpha_t)$. Therefore, at low angle of attack it takes a substantial contribution from the ϕ' motion to negate the lateral motion. ***Nevertheless, the combinations shown in*** Table 3-4 ***are acceptable for high total-angle-of-attack-applications.***

An alternative set of superposition results are given in Table 3-5. Note that these alternates are made possible because, unlike the others, the pitch and yaw characteristic motions require translational velocities in ***both*** the lateral and "vertical" directions. They were derived by negating the *y*-velocity component of the pitching motion with the yawing motion and vise

versa (at the expense of an increased z velocity). This, the only remaining translational velocity component, was then canceled by a contribution from the α_t characteristic motion.

Motion	$\bar{q}$	$\bar{r}$	$\overline{\Delta\alpha_t}$	$\dot{\alpha}_t$
Pitch	$\bar{q}$	$-\tan(\phi_0')\bar{q}$	$\dfrac{\bar{q}}{\omega\cos(\phi_0')}$	$\dfrac{q}{\cos(\phi_0')}$
Yaw	$-\cot(\phi_0')\bar{r}$	$\bar{r}$	$\dfrac{-\bar{r}}{\omega\sin(\phi_0')}$	$\dfrac{-r}{\sin(\phi_0')}$

Table 3-5 Alternative Interpretation for Rectilinear Motion

Rectilinear motion for the pitch case, interpreted in this way, is much improved over the entire angle of attack range. The only problem is a singularity at a roll angle of 90 degrees. Unfortunately, the resulting rectilinear motion for a yawing motion has its singularity for the symmetric flight condition $\phi_0' = 0$, the situation most often of interest. This poses no difficulty for configurations that are sufficiently symmetric, e.g., a cruciform missile. In that case, the aerodynamic characteristics for pitch and yaw are identical and the yawing motion is superfluous.

The pitching motion results presented in Table 3-5 are interesting, though. Recall that the rotation rates are body-axis rates and $\bar{r} = -\bar{q}\tan(\phi_0')$, i.e., the rotation-rate vector $\bar{q}$ is directed along the y_b axis and $\bar{r}$ is in the $-z_b$ direction. Therefore, the angle from $\bar{q}$ to the vector sum of $\bar{q}$ and $\bar{r}$ is

$$\tan^{-1}\left(\frac{\bar{r}}{\bar{q}}\right) = \tan^{-1}\left(\frac{-\bar{q}\tan(\phi_0')}{\bar{q}}\right) = -\phi_0'$$

and the magnitude of the resultant is

$$\frac{\bar{q}}{\cos(\phi_0')}$$

Therefore, a rectilinear motion with a pitching rate of this magnitude about the y_t axis will produce the motion specified in Table 3-5. Figure 3-6 depicts the geometry, looking forward along the positive x_b axis.

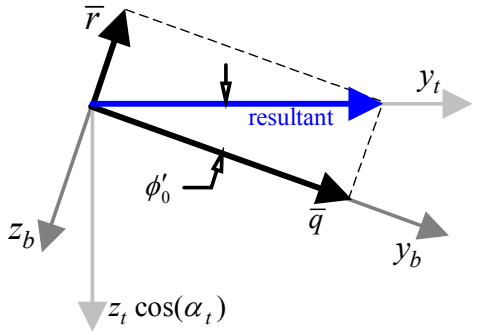

Figure 3-6 -- Rotation-Rate Vectors for Pitching Motion

This could be quite important because the wind-tunnel facility may not be able to provide a body-axis pitching motion for $\phi_0' \neq 0$. We should note however, that not all wind-tunnel dynamic rigs are single degree-of-freedom devices. Furthermore, of those that are SDOF, not all are exclusively rotational rigs, some can provide translational motions. If there are special requirements to be met, it would be wise to determine if a facility is available that can provide what is needed.

4 Data Reduction

In theory, extracting the stability derivatives from wind tunnel test data is not difficult. The previous sections provide the background required for this task; we know physically what we are attempting to measure, the motions of the vehicle relative to the air-stream that we are likely to encounter, and that we may have to settle for measurements involving combinations of the desired quantities rather than independent measurements for each. However, this task must be accomplished in the presence of other undesirable effects. These issues are addressed in this section.

4.1 Harmonic Motion Inputs

Almost all facilities that have dynamic testing equipment use harmonic motions (about the various axes) as the basis for dynamic derivative measurement. For the most part, these are referred to as inexorably forced oscillation techniques. That is, the motion is mechanically constrained (sometimes in combination with a feedback control system) to be a harmonic oscillation ***that is independent of the aerodynamic loads*** acting on the test model. The loads are measured with a strain-gage balance mounted between the model and sting.

Other methods have been used. One example is the free-oscillation technique where the model is free to rotate about a given axis, perhaps on an air bearing. The model is given an initial angular displacement and the motion's decay is observed as a function of time. Assuming a linear air reaction, the rate of decay can be related to the dynamic stability derivative ("damping derivative") describing the aerodynamic ***moment*** due to rotation rate about that axis. This technique has disadvantages: the frequency of oscillation is dependent on the model's inertia and, of course, the model must be statically stable, otherwise the motion will simply diverge aperiodically.

In a modification of the free oscillation technique, the model is connected to the sting through a "flexure" or torsion spring. Again the decay rate is related to the dynamic derivative. This solves the problem with a statically unstable configuration, however, the flexures and model inertia must be tailored to obtain data over a suitable frequency range and it gives only information about the aerodynamic moment.

Yet another involves a flexure, a means for applying an excitation force to the model, and a control system to vary the excitation in order to maintain constant amplitude. In this case, the energy required to hold the amplitude constant can be related to the damping derivative.

A direct measurement of the forces and moments is not made with any of these alternatives and they have largely fallen into disfavor. Only data reduction techniques for the inexorably forced oscillation case are discussed below.

4.2 Data Processing

Strain-gage balance signals consist of voltages* that are proportional to the desired aerodynamic loads plus inertia forces and moments due to the motion (including sting vibration). In addition, it contains electrical noise and, in the case of a system that has analog-to-digital elements, is modified by the presence of anti-aliasing filters.

So the unwanted contributions must be "stripped" from the total signal. To this end, the model needs to be made as light as possible (while meeting structural integrity requirements), thus maximizing the signal-to-noise ratio. (We do not want the aerodynamics to be "swamped" by the inertial loads.)

By far the most common method for removing the inertia loads is through the use of "tare runs", i.e., dynamic tests performed "wind-off." Here, the assumption is that the model motion under wind-on conditions can be replicated wind-off. The measured loads are assumed to be only due to inertial reactions. However, this is never quite true, especially if the motion is controlled with a feedback control system. There may be very good control over the angular position, but errors in the rotation rate and acceleration are generally larger. Therefore, the "aggressive" elimination of position errors can lead to

* The tunnel system will provide signal processing that applies balance calibration equations to give voltages that can be interpreted in terms of physical quantities. Cross talk between the force and moment channels is minimized in this process.

differences in wind-on and wind-off inertial loads* (simply because the loading time histories are different). Even if the motions repeat well, excitation of the sting vibration modes will differ when air loads are present.

Measurements taken in the VWT are shown below. The motion was a harmonic body-axis roll, and we will be working in the aeroballistic axes. A roll-angle time history, the digital signal from an optical encoder mounted at the base of the sting, is shown in Figure 4-1. Note that this ***is not*** the motion at the model station because of sting flexibility. Test conditions were $q_\infty = 3$ psf, $\alpha_{t_0} = 10°$ and $\phi_0' = 0$. The test frequency was 0.24 Hertz.

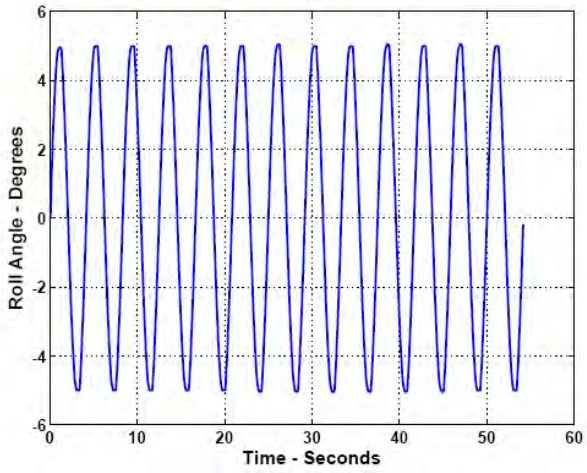

Figure 4-1 Rolling Motion vs. Time

A time history of the rolling moment for this motion (recorded during a tare run) is presented in Figure 4-2. Clearly, even in the wind-off case, the signal is quite noisy. Rolling-moment data for the corresponding wind-on test run are plotted in Figure 4-3. Note that the motion's periodicity is more evident (because of the periodic nature of the aerodynamic moment) even in the presence of the noise.

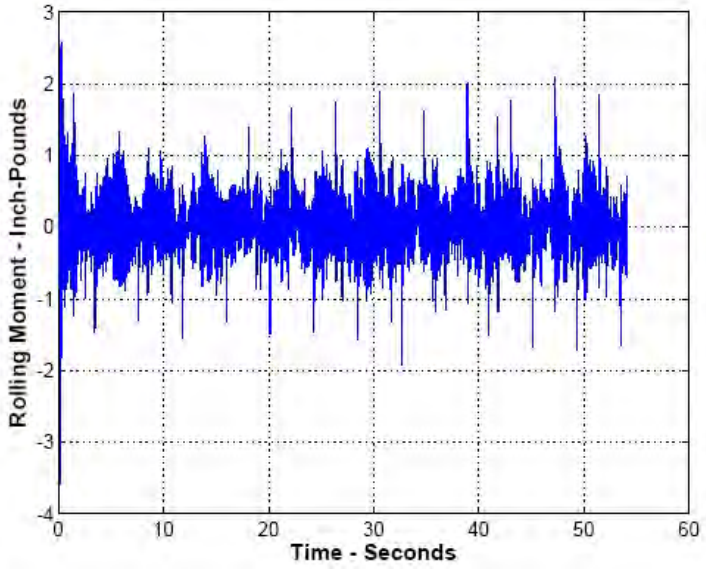

Figure 4-2 Rolling Moment Tare

* Control systems can be designed to minimize these difficulties by including rate feedback in various ways. The VWT is very good in this respect, providing excellent motion repeatability (even at the acceleration level).

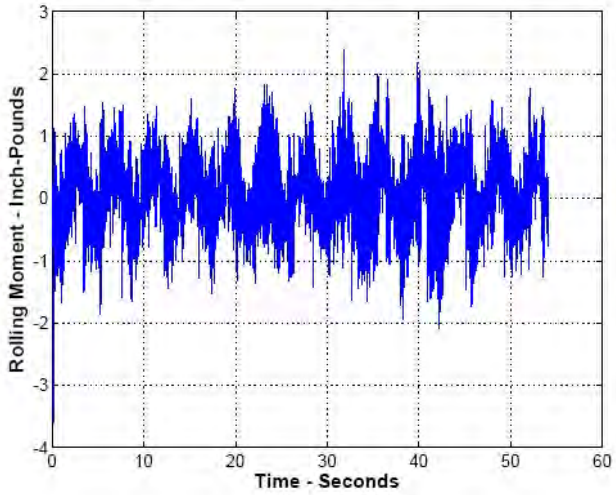

Figure 4-3 Rolling Moment - "Wind On"

The inertial contribution is removed by simply subtracting the tare from the measured values, point by point, with the result shown in Figure 4-4. Even though the periodic nature of the aerodynamic response is clearly evident, we would be hard pressed to extract any meaningful stability derivatives from data in this form. There are a couple of ways to proceed at this point.

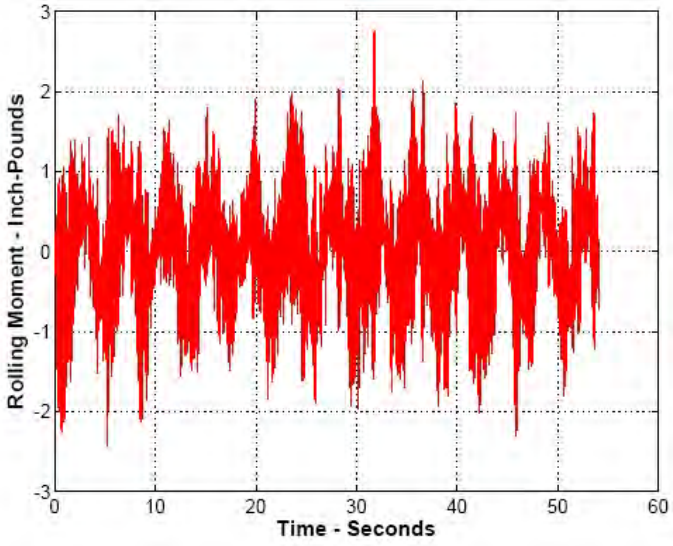

Figure 4-4 "Aerodynamic" Rolling Moment

One option is to filter the data, leaving primarily the response at the forcing frequency. However, this approach has several drawbacks. First, care must be taken in selecting the filtering algorithm. In general, filtering introduces phase lags* and the phase relationship between the motion and the aerodynamic response is important. Second, the frequency response for all of these filters is never perfectly "flat" up to the cut-off frequency and "roll-off" characteristics at frequencies above the cut-off vary. So filtering never completely eliminates the noise while (at the same time) leaving the desired signal unaltered. Also, filtering introduces an initial transient that requires some of the data to be discarded. Finally, even though a linear system can respond only at the forcing frequency, in nonlinear situations what is, or is not, noise may not be so clear.

For reasons that will become apparent, the author prefers accomplishing this task in the frequency domain. Our basic tool will be the Fast Fourier Transform (FFT).

* For post-processing applications "zero-lag" filter algorithms are available.

4.2.1 Fourier Transforms

Fourier transforms are an extension of the familiar Fourier series (written in complex form) often used as an alternate means of representing a periodic function of time. Given such a function, $f(t)$, with period $2T$, its Fourier series is written

$$f(t) = \frac{a_0}{2} + \sum_{k=1}^{\infty} a_k \cos(\Omega_k t) + b_k \sin(\Omega_k t) \qquad 4\text{-}1$$

in which

$$a_k = \frac{1}{T}\int_{-T}^{T} f(t)\cos(\Omega_k t)\,dt$$

$$b_k = \frac{1}{T}\int_{-T}^{T} f(t)\sin(\Omega_k t)\,dt$$

$$\Omega_k = k\frac{\pi}{T}$$

$$k = 0, 1, 2, \ldots, \infty$$

This can be written more compactly in complex form. The details of the derivation will not be repeated here and can be found in almost any standard text. But the idea is to use Euler's formula

$$e^{\pm i\Omega t} = \cos(\Omega t) \pm i\sin(\Omega t)$$

to write the sine-cosine pairs in Equation 4-1 in complex form, i.e.,

$$a_k \cos(\Omega_k t) + b_k \sin(\Omega_k) = \frac{1}{2}(a_k - i\,b_k)e^{i\Omega_k t} + \frac{1}{2}(a_k + i\,b_k)e^{-i\Omega_k t}$$

After some manipulation, it can be shown that

$$f(t) = \frac{1}{2T}\sum_{k=-\infty}^{\infty} F(\Omega_k)e^{i\Omega_k t} \qquad 4\text{-}2$$

where

$$F(\Omega_k) = \int_{-T}^{T} f(t)e^{-i\Omega_k t}\,dt \qquad 4\text{-}3$$

Thus the periodic (not necessarily harmonic) function $f(t)$ is expressed as a linear combination of harmonic functions of time. Note that the sequence of frequencies is discrete, i.e., each frequency is an integer multiple of the "fundamental" frequency, $2\pi/2T$. Also, the "cost" of obtaining this concise form is that the complex conjugates of $F(\Omega_k)$ are needed. They are provided by including negative frequencies in the summation, i.e., the integer k now runs from $-\infty$ to ∞.

Note that the signs on the exponents are a matter of convention; the description given here is the one normally used in engineering. However, the only requirement is that the exponents of the transform and its inverse are opposite in sign. $F(\Omega_k)$ is a complex number giving the amplitudes of the cosine (real part) and sine (imaginary part) terms of the k^{th} harmonic component.

We can think of $F(\Omega_k)$ as a vector when plotted in the complex plane, as shown in Figure 4-5. That is, it can also be written in the form

$$F(\Omega_k) = \left|F(\Omega_k)\right| e^{i\varphi}$$

where

$$\varphi = \tan^{-1}\left(\frac{\mathrm{Im}\left(F(\Omega_k)\right)}{\mathrm{Re}\left(F(\Omega_k)\right)}\right) \qquad 4\text{-}4$$

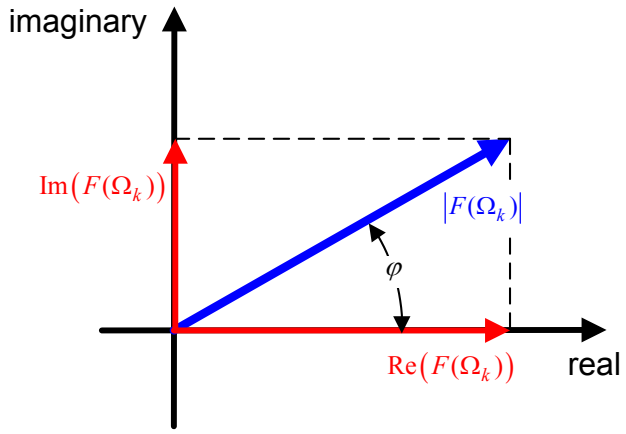

Figure 4-5 Harmonic Component in the Complex Plane

The time-varying nature of $f(t)$ is provided by considering the vectors $F(\Omega_k)$ to be rotating at a constant angular velocity, Ω_k. Each has a contribution at time "t" that is given by its projection onto the real axis, as shown in Figure 4-6. Initially, the projection of a positive imaginary part of $F(\Omega_k)$ produces a negative $f(t)$. Therefore, a function $f(t) = A\sin(\Omega t)$ will have a negative imaginary part and the real part will be zero.

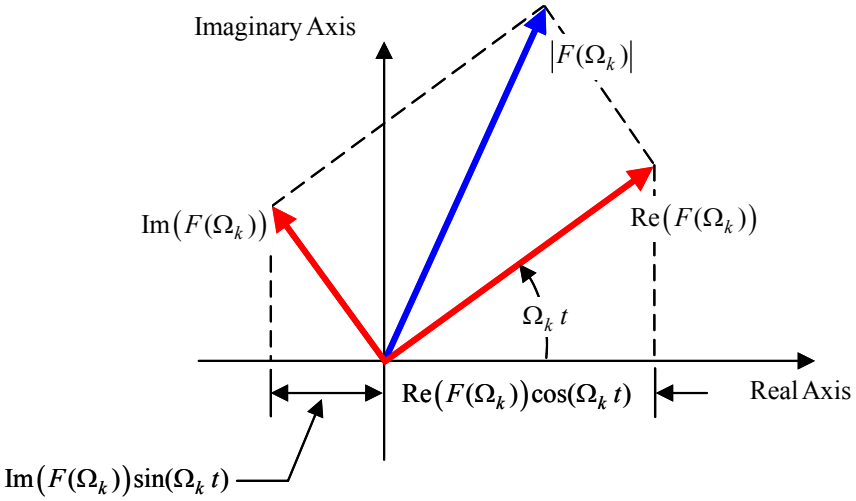

Figure 4-6 Spectral Component's Contribution to *f(t)*

If the function $f(t)$ is not periodic, its "period" ($2T$), approaches infinity, the increment between two successive frequencies ($\Delta\Omega = \Omega_{k+1} - \Omega_k = \frac{\pi}{T}$) must approach 0 and the frequency spectrum becomes continuous. Therefore, Equations 4-2 and 4-3 can be rewritten as

$$f(t) = \frac{1}{2\pi}\int_{-\infty}^{\infty} F(\Omega)e^{i\Omega t}d\Omega \qquad 4\text{-}5$$

and

$$F(\Omega) = \int_{-\infty}^{\infty} f(t)e^{-i\Omega t}dt \qquad 4\text{-}6$$

Equations 4-5 and 4-6 form a transform pair. $F(\Omega)$ is the Fourier transform of $f(t)$, and $f(t)$ is the inverse Fourier transform of $F(\Omega)$.

For sampled data, the Discrete Fourier Transform (DFT) is used. It is simply the Fourier transform, put into discrete form and the FFT is an efficient algorithm for computing the DFT. However, the finite data range, implicitly assumes that $f(t)$ has a period equal to the length of the record. The DFT covers the frequency range $-\frac{f_s}{2}$ to $\frac{f_s}{2}$, where f_s is the sampling frequency. The frequency spectrum is divided into frequency "bins" and the width of each bin is determined by the number of samples in the time record. Therefore, the accuracy with which a given spectral component is known (as a function of frequency) depends on the number of points in the data set (n_{pts}), i.e., it depends on the product of the sampling rate and record length (in time). Furthermore, the FFT algorithm requires no knowledge of either time or frequency. Therefore, a meaningful frequency spectrum must be computed based on the data in hand. For the positive part of the spectrum

$$f_k = f_s \frac{k}{n_{pts}} \qquad k = 0,\ 1,\ 2,\ldots \frac{n_{pts}}{2} \quad \text{if } n_{pts} \text{ is even}$$

or

$$f_k = f_s \frac{k}{n_{pts}} \qquad k = 0,\ 1,\ 2,\ldots \frac{n_{pts}-1}{2} \quad \text{if } n_{pts} \text{ is odd}$$

The "zero frequency" value of $F(\Omega)$ corresponds to the term $\frac{a_0}{2}$ in Equation 4-1 and is equal to one-half the function's mean value over the length of the record. By convention, only the positive half, including zero, of the spectrum is displayed (or plotted); the negative half of the spectrum is the complex conjugate of the corresponding element on the other side. Of course, the full spectrum must be used when computing the inverse.

4.2.2 Data in the Frequency Domain

VWT data previously presented in Figure 4-1 (motion) and Figure 4-4 (aerodynamic moment) are reviewed below from the frequency domain perspective. The sample rate was 100 Hz. for both*. Figure 4-7 provides plots of the real and imaginary parts of the roll-angle DFT. (The roll-angle axes of the plots are half spectrums scaled up by a factor of two).

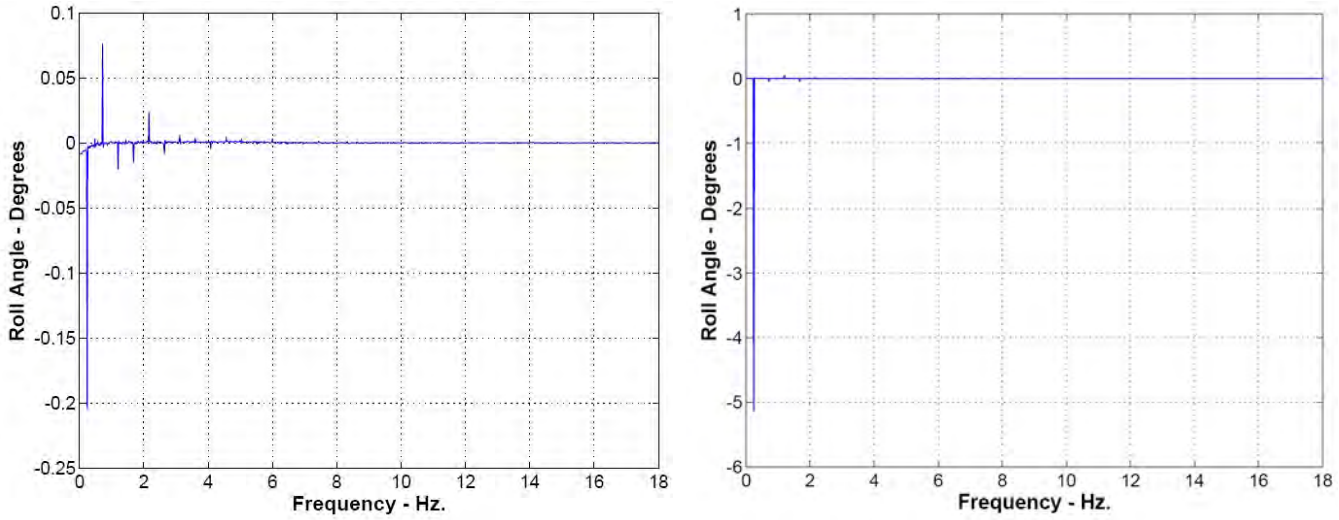

(a) Real Part **(b) Imaginary Part**

Figure 4-7 Rolling Motion in the Frequency Domain

* In the VWT, the roll angle as seen by the encoder is actually sampled at 500 Hz. because it is used as a part of the motion control system. In extracting stability derivatives from the raw data, it is good practice to keep the frequency bins for both the motion and strain-gage balance output the same size. Therefore, the roll-angle record was "sub-sampled".

Note the difference in roll-angle scales between the real and imaginary parts. The motion is a very clean 5 degree amplitude sinusoid at 0.24 Hz. as seen by the large spikes there.* We know that it is a sinusoid because its imaginary part is dominant and negative, see Figure 4-6. Also, from Equation 4-4, $\varphi \cong -92.3°$ (the result is in the third quadrant, negative numerator and negative denominator) so the motion lags a pure sine wave by about 2.3 degrees†.

An aerodynamic rolling-moment DFT for this motion is plotted in Figure 4-8 (the corresponding time-history is shown in Figure 4-4). The response at the forcing frequency is unmistakable, and $\varphi \cong 117.1°$. Note that there are vibration modes (with this model/sting combination) in the 14-16 Hz. range that cannot be detected by the encoder at the aft end of the sting but contribute to the inertial loads sensed by the balance. These inertial loads differ between the wind-on and wind-off cases and therefore are not totally removed by subtracting the tares, note the "noise" evident in the time domain plot (Figure 4-4).

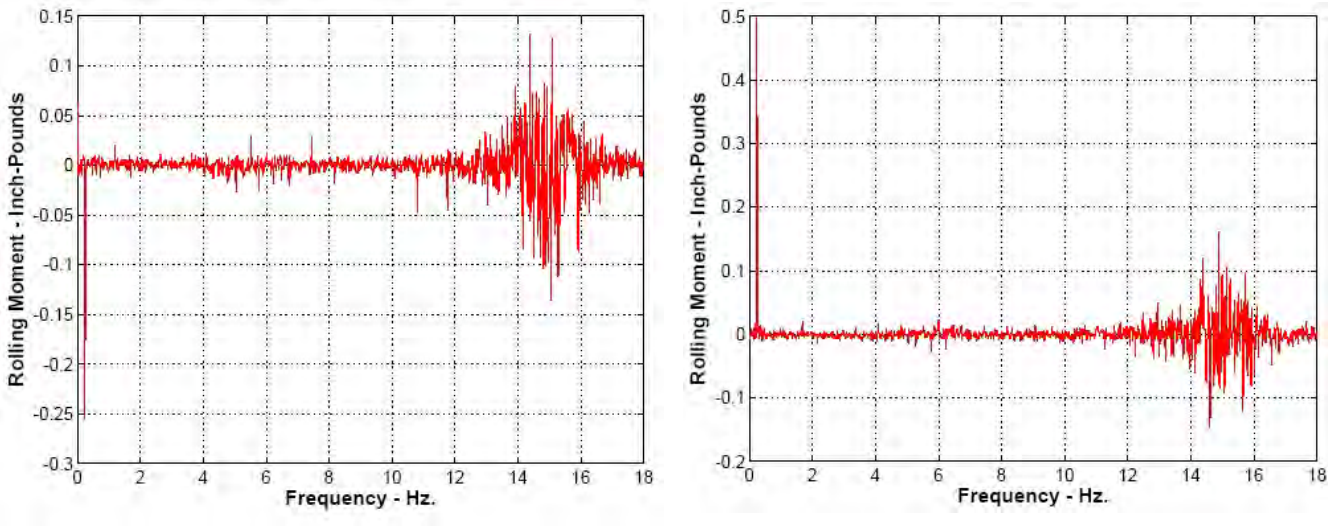

(a) Real Part **(b) Imaginary Part**

Figure 4-8 Aerodynamic Rolling Moment in the Frequency Domain

4.2.3 Extracting the Stability Derivatives

Referring to Table 3-4, the aerodynamic rolling moment is assumed to have the form

$$L = L_0 + L_{\phi'}\,\phi' + L_p\,p + L_{\dot{\phi}'}\,\dot{\phi}' \qquad 4\text{-}7$$

where

$\phi' = \bar{\phi}' \sin(\omega t + \varphi_1)$

$p = \bar{\phi}'\,\omega \cos(\omega t + \varphi_1)$

$\dot{\phi}'$ is numerically equal to p

and

φ_1 is an arbitrary phase angle for the motion that depends only on the time reference for the experiment

* If you can read the frequency scale on these plots that well, you are pretty good. However, that is where they really are.

† This lag in itself is not important since it depends on an arbitrary time reference. What ***is*** important is the phase relationship between the motion and the aerodynamic reaction.

Thus, the rolling moment is given by

$$L = L_0 + L_{\phi'}\,\phi' + \left(L_p + L_{\dot{\phi}'}\right)\dot{\phi}' \qquad 4\text{-}8$$

In our case, L and ϕ' are known harmonic functions of time (better yet, their discrete Fourier transforms are readily found even if buried in noisy data) and we need to solve for the unknown stability derivatives. Of course, as before, the transforms can be thought of as rotating vectors plotted in the complex plane. Arbitrarily choosing to view them at $t = 0$, we have

$$\mathbf{F}\left(\{L\}\right)_k = \bar{L}_k\, e^{i\varphi_{2_k}}$$

$$\mathbf{F}\left(\{\phi'\}\right)_k = \bar{\phi}'_k\, e^{i\varphi_{1_k}}$$

and

$$\mathbf{F}\left(\{\dot{\phi}'\}\right)_k = \mathbf{F}\left(\{p\}\right)_k = \bar{\phi}'_k\, i\,\omega_k\; e^{i\varphi_{1_k}}$$

where

$\mathbf{F}\left(\{x\}\right)_j$ denotes the j^{th} element of the DFT of the array "x"

$\omega_k = 2\pi f_k =$ the forcing "circular" frequency $\left(\text{rad/sec}\right)$

φ_1 and φ_2 are phase angles for the motion and rolling moment respectively as defined in Equation 4-4

If the time-domain arrays have *n* points, their frequency-domain counterparts will have either $\frac{n+1}{2}$ *or* $\frac{n}{2}+1$ points, depending on *n* (odd or even) in the positive half of the frequency domain.

Now, taking the DFT of Equation 4-8* and looking at its k^{th} element

$$\bar{L}\, e^{i\varphi_2} = L_{\phi'}\,\bar{\phi}'\, e^{i\varphi_1} + \left(L_p + L_{\dot{\phi}'}\right)\bar{\phi}'\, i\,\omega\; e^{i\varphi_1}$$

where

the index *k* has been dropped for simplicity

Dividing both sides by $\bar{\phi}' e^{i\varphi_1}$

$$\frac{\bar{L}}{\bar{\phi}'} e^{i(\varphi_2 - \varphi_1)} = L_{\phi'} + \left(L_p + L_{\dot{\phi}'}\right) i\,\omega$$

And finally, we have

$$L_{\phi'} = \mathrm{Re}\left(\frac{\bar{L}}{\bar{\phi}'} e^{i(\varphi_2 - \varphi_1)}\right) \qquad 4\text{-}9$$

and

$$L_p + L_{\dot{\phi}'} = \frac{1}{\omega}\,\mathrm{Im}\left(\frac{\bar{L}}{\bar{\phi}'} e^{i(\varphi_2 - \varphi_1)}\right) \qquad 4\text{-}10$$

Importantly, the portion of the rolling moment response that are associated with the static and dynamic "stability derivatives" respectively is determined by phase-angle difference between the motion and the aerodynamic response. This could have been anticipated since we know that the dynamic "derivatives" are first order approximations for the time required for the indicial response to reach its steady state response. If the aerodynamic response is very "fast" then $\varphi_2 - \varphi_1$ is small leading to numerical accuracy (small difference) problems, i.e. the phase angle difference is less precise than either of the phase angle measurements individually.

* The constant term, L_0, is the first element (index equals zero) of the transform.

It is useful to put these in a different form. $\bar{L}e^{i\varphi_2}$ and $\bar{\phi}'e^{i\varphi_1}$ are the discrete Fourier transforms of the measured rolling moment and roll angle respectively, both evaluated at the forcing frequency. Thus, Equations 4-9 and 4-10 may be rewritten

$$L_{\phi'} = \mathrm{Re}\left(\frac{\mathbf{F}\left(\{L\}\right)_k}{\mathbf{F}\left(\{\phi'\}\right)_k} \right) \qquad 4\text{-}11$$

and

$$L_p + L_{\dot{\phi}'} = \frac{1}{\omega}\mathrm{Im}\left(\frac{\mathbf{F}\left(\{L\}\right)_k}{\mathbf{F}\left(\{\phi'\}\right)_k} \right) = \frac{1}{2\pi f_k}\mathrm{Re}\left(\frac{\mathbf{F}\left(\{L\}\right)_k}{i\mathbf{F}\left(\{\phi'\}\right)_k} \right) = \frac{-1}{2\pi f_k}\mathrm{Re}\left(\frac{i\mathbf{F}\left(\{L\}\right)_k}{\mathbf{F}\left(\{\phi'\}\right)_k} \right) \qquad 4\text{-}12$$

Of course, any of the relationships for $L_p + L_{\dot{\phi}'}$ in Equation 4-12 may be used at the convenience of the analyst.

No assumptions regarding the existence of stability derivatives were made in this development. However, the mathematical form of the rolling-moment response, Equation 4-8, ***was*** assumed (the procedure is valid whether this relationship is interpreted as an asymptotic expansion or as a Taylor series). If the assumptions underpinning Equation 4-8 are not valid, we must resort to other means of modeling the rolling-moment response.

Figure 4-9 is a plot of Equation 4-11 over a range of frequencies. It covers a range of indices that includes "*k*" (the index for the motion's dominant frequency). The ratio at the forcing frequency *k*, i.e., the one representing $L_{\phi'}$, is indicated by the red circle.

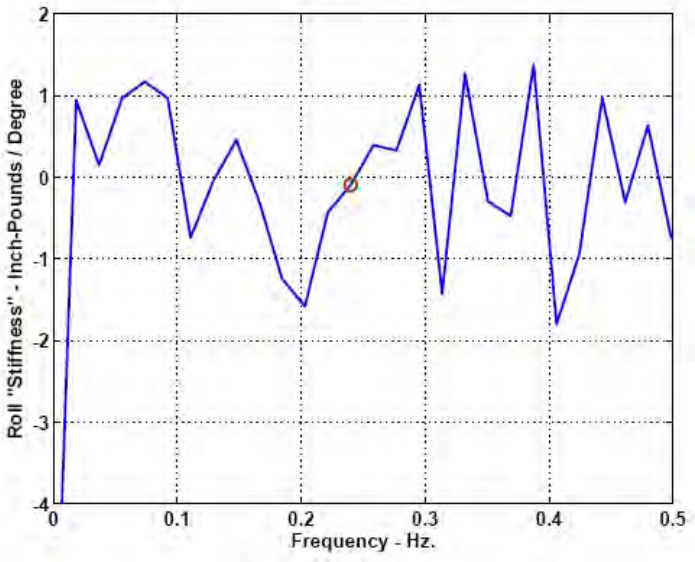

Figure 4-9 Roll "Stiffness" Derivative, $L_{\phi'}$

Note that ratio takes on a wide range of values in this frequency range. Even though the numerator is small, the denominator (except at the forcing frequency) is small also (since there is essentially no motion at the other frequencies, see Figure 4-7). Needless to say, the value at $f = 0.24$ is the only one to be trusted.

Similarly, results from Equation 4-12 are plotted in Figure 4-10. The "derivative" contains the combined effects of rotation and translation $L_p + L_{\dot{\phi}'}$ due to the rectilinear motion in the tunnel. Again, the answer we are looking for is indicated by the red circle.

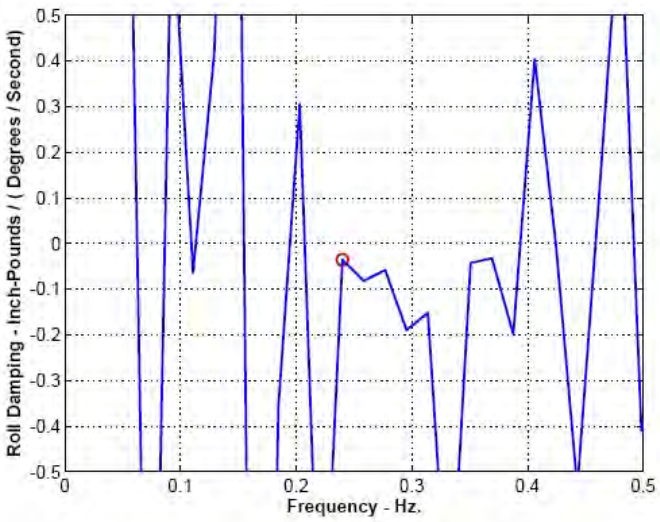

Figure 4-10 Roll Damping Derivative

Referring to the discussion regarding Equation4-10, the accuracy of the damping derivative computation directly related to the measured difference between the two phase angles. In the present case, $\varphi_2 - \varphi_1$ = 209.4 degrees. The sensitivity of $L_p + L_{\dot{\phi}'}$ determination from Equation 4-12 to phase-angle errors can be shown to be

$$\varepsilon_\varphi = \frac{d\left(L_p + L_{\dot{\phi}'}\right)}{d\left(\varphi_2 - \varphi_1\right)} = \frac{1}{\omega}\frac{\bar{L}}{\bar{\phi}'}\cos(\varphi_2 - \varphi_1) = -2.043 \ \frac{\text{inch-lbs sec}}{\text{rad}^2}$$

$$= -0.036 \ \frac{\text{inch-lbs sec}}{\text{rad}}\frac{1}{\text{deg}}$$

Note that $\cos(\Delta\varphi) = -\cos(\Delta\varphi - 180)$ when the result falls in the third quadrant. This will usually be the case, i.e., for a configuration that is both statically and dynamically stable in roll. Thus, for this example, the relevant phase difference is about -39 degrees (the minus sign simply means that $L_{\phi'}$ is negative and the dynamic response lags the motion by an additional 39 degrees). We would not expect severe accuracy problems in this case.

The sensitivity expressed in terms of percentage change is given by:

$$\frac{\varepsilon_\varphi}{L_p + L_{\dot{\phi}'}} = \cot(\varphi_2 - \varphi_1)\ \frac{1}{\text{rad}}$$

So for our example, the error in the damping derivative is about 3.1% for each degree of phase error.

Maximum sensitivity occurs when $\varphi_2 - \varphi_1$ is either 0 or π radians (and in absolute terms would be about double that given above for the example's phase angle). Furthermore, this corresponds to the no damping case (which is why the percentage error "blows up"). An error in phase determination of a few degrees here can make the difference between dynamic stability and a significant instability.

Extracting the other derivatives (for this and different motions) is accomplished in the same manner. Note that there are time-domain procedures for extracting the dynamic stability derivatives. However, clean signals are required and the technique presented here avoids the need to filter the data. Furthermore, we get estimates for both the static and dynamic derivatives, both of which are obtained under dynamic conditions. As we will see in Section 5 this can provide a vital check on the validity of using Equation 4-7 as an appropriate model for the aerodynamic reaction.

5 Indicators that things are going right (or wrong)

In view of the discussions of the stability derivative concept's inherent limitations (Section 2.4) and those regarding the form of Equation 4-7, good practice dictates that we ensure that the extracted stability derivatives are valid. Fortunately, there are several convenient ways of doing this.

5.1 Properties of Linear Aerodynamic Systems

Recall that all of the procedures discussed assume that the aerodynamic response is linear. As we have seen though, the stability derivative model can fall apart even if the response is linear, e.g., with motions that were not "slow enough". We begin the present discussion with an issue that is perhaps intuitively obvious.

5.1.1 Amplitude and Frequency Dependency

A well-planned test should include a series of "runs" at fixed steady-state flight conditions, at a constant reduced frequency and that cover a range of motion amplitudes. Care should be taken to ensure that the selected amplitudes stay within the anticipated linear range and to ensure that the reduced frequency is in the range of expected flight values. The same should be done holding amplitude constant over a range of reduced frequencies.

Equations 4-11 and 4-12 tell us what we should know already, i.e., they are the real and imaginary parts of aerodynamic transfer functions* for rolling moment due to roll-angle and roll-rate, respectively (evaluated at $s = i\omega$). Said another way, they are the aerodynamic system's frequency response, evaluated at the forcing frequency. If either of these two "derivatives" shows a dependency on amplitude (barring experimental scatter), nonlinear effects are present because a linear time-invariant system must have a unique transfer function.

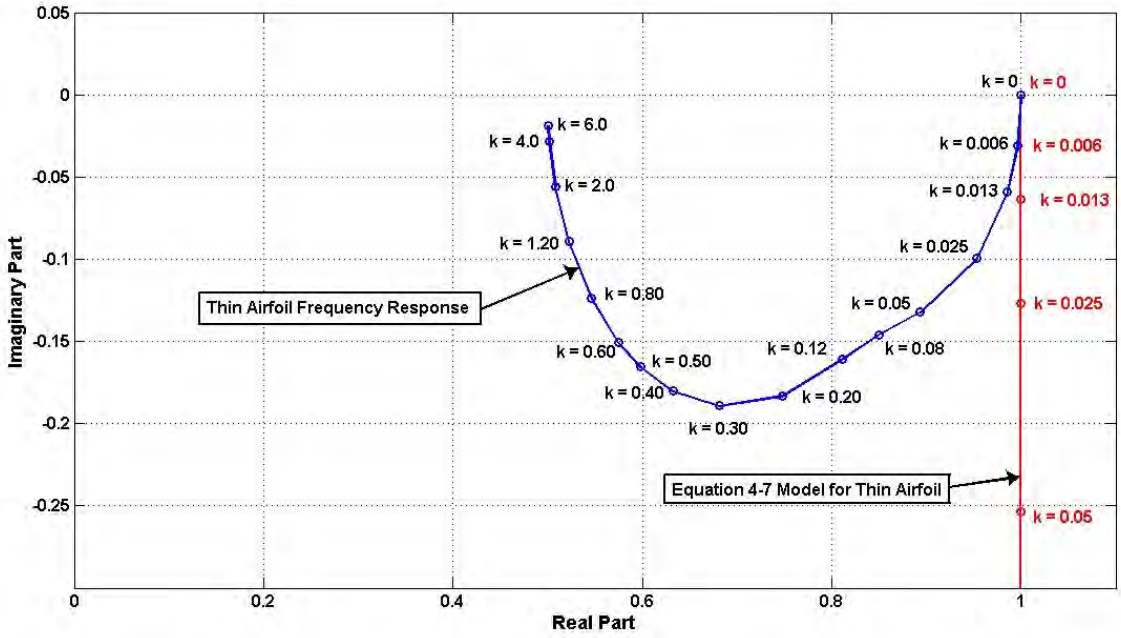

Figure 5-1 -- Thin Airfoil Frequency Response vs. Stability "Derivative" Model

A linear system's output can depend on the frequency of the input, as we saw in Section 2.4.4. However, ***stability derivatives cannot***. An example (the linear unsteady response of a thin airfoil in an incompressible fluid) is shown in Figure 5-1. The airfoil's frequency response (Theodorsen's function) is plotted in blue. Recall that the real part of the frequency response

* Transfer functions can be formed using the Fourier transform. However, transfer functions expressed in the frequency domain cannot capture transient behavior.

function is that portion of the response (normalized by the static lift-curve slope) that is in phase with the motion. The imaginary part is 90 degrees out of phase with the motion (a negative value indicating a lagging response). A perfectly executed experiment would follow the blue curve as a function of reduced frequency (k). As shown in the figure, the in-phase component decreases monotonically with increasing frequency, dropping to about 68% of the static value at k = 0.3, and asymptotically approaching 50% at very high reduced frequencies. On the other hand, the frequency response function corresponding to Equation 4-7 is given by

$$1 - ik\int_0^\infty F(\hat{t})\,d\tau$$

where

$F(\hat{t})$ is the system's deficiency function

For the two-dimensional airfoil the deficiency function is given by Wagner's function, yielding

$$C_{L_\alpha}(k) = 1 - 5.071ik$$

This model is plotted in red. Notably, Equation 4-7 insists that the in-phase component (the real part) is independent of frequency and never deviates from the true static value. Furthermore, the quadrature component is directly proportional to the reduced frequency. Therefore the damping "derivative" is also independent of frequency as shown by Equation4-12.

So if either (or both) derivatives show significant frequency effects we cannot be sure of the cause, but the aerodynamic response is surely too slow to be adequately represented by Equation 4-7 and there may (or may not) be nonlinearities present. Just how much variation is acceptable, is a matter of engineering judgment. A convenient way of making this assessment is discussed in the following section.

5.2 "Static" Derivative Agreement (Dynamic tests vs. "True" Static Values)

A static test should always precede the dynamic test because of its value in interpreting dynamic test results and because it can be a tremendous aid in laying out an effective test plan. If there are significant differences between the static test results and those extracted under dynamic conditions something is going wrong (see the discussion above).

The following check should give good results, even in the presence of mild nonlinearities in the static data. Lift coefficient changes with angle of attack serves as our example. (Application to any other static force/moment coefficient is straight forward.)

1. Plot the statically measured C_L vs. α
2. Compare with:

$$C_L(\alpha_0 \pm \overline{\Delta\alpha}) = \left[C_L(\alpha_0)\right]_{stat} \pm \left[C_{L_\alpha}\right]_{dyn} \overline{\Delta\alpha} \qquad 5\text{-}1$$

where:

α_0 ..... mean value of α for the dynamic test run

$\overline{\Delta\alpha}$ ..... amplitude of the dynamic test run

$\left[C_L(\alpha_0)\right]_{stat}$ ..... lift coefficient from the static tests, evaluated at α_0. Interpolate if necessary, although with a well planned test this shouldn't be needed. As a last resort use the mean value of C_L from the dynamic test run (if nonlinearities exist, the mean can contain a bias, see the discussion below).

$\left[C_{L_\alpha}\right]_{dyn}$ ..... lift curve slope as determined from the dynamic test, i.e., the real part of the C_L to α transfer function evaluated at the forcing frequency.

Note that a simple plot of the derivatives (determined from the dynamic test) vs. frequency and amplitude can be sufficient. However, the suggested procedure allows an informed judgment to be made based on the slope of the static curve and the amount of scatter present in the data.

The procedure is illustrated in the following four figures. Static data, taken in the VWT, are shown in Figure 5-2.

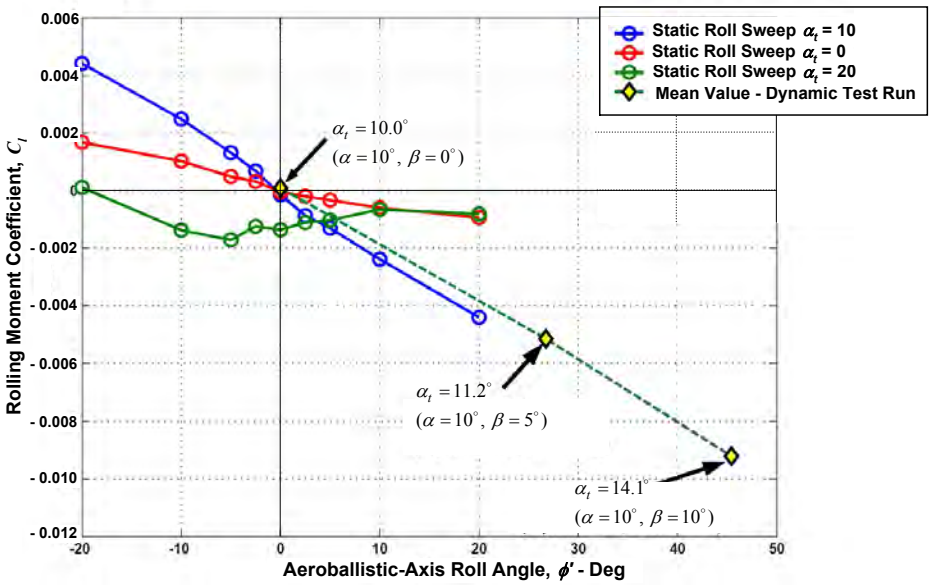

Figure 5-2 Static Rolling Moment Data from the VWT

Three roll sweeps (at $\alpha_t = 0^\circ, 10^\circ$ and 20°) are shown, in addition to three points that actually came from harmonic tests. The latter assume that the correct static value (at each condition) is given by the mean value of the measured loads over the length of the dynamic run. This may or may not be true because any component of the rolling moment that is proportional to an ***even power*** of the instantaneous roll angle will also produce a bias in the rolling moment's mean value. All such terms introduce a second harmonic response; therefore, a check of the rolling moment DFT (for a second harmonic spike) will reveal the presence of any significant bias producing terms. In this case, there are none, and the mean value should be a reasonable estimate of the true static value.

Figure 5-2 shows the difficulties that can be encountered if the test plan is not thought out completely. The primary objective of the test was to gather rolling motion data at conditions where nonlinearities play a significant role. Aeroballistic axes were the natural choice for these experiments. However, for reasons not directly related to primary effort, roll damping data were desired over a range of angle of attack and sideslip combinations. Since the static roll sweeps (in the aeroballistic system) did not cover a range equivalent to the array of α and β needed for the roll damping tests, static data were not available for interpolation. Even if the range was sufficient, interpolation would still have be difficult since there are only three values of α_t available and a severe nonlinearity appears somewhere between 10 and 20 degrees.

Using mean values of the dynamic runs as a substitute for true static values, the effects of motion amplitude and frequency are presented in Figure 5-3 and Figure 5-4. The variations about the mean* due to amplitude and frequency are shown by the green, red and blue "dumbbells." Mean values are shown by the yellow diamonds.

In Figure 5-3 Amplitude Effects on "Static" BehaviorFigure 5-3 amplitudes up to 10 degrees agree quite well with the "true" static data for the motion about $\phi' = 0^\circ$, $\alpha_t = 10^\circ$. Such is not the case at $\phi' \cong 27^\circ$. However, this test was performed at a total angle of attack of 11.2 as opposed to the 10 degrees for the static roll sweep. Based on Figure 5-2 we are hard pressed to identify which side of the $\alpha_t = 10^\circ$ curve we would expect the true static data to fall. If the dashed green line (straight-line connectors between the dynamic mean values) represents a good approximation to the actual static points, amplitude effects

* Obtained from Equation 5-1 adapted to $C_{l_{\phi'}}$ and ϕ' instead of C_{L_α} and α.

are fairly small. Some nonlinearity probably exists. The systematic decrease in slope, with increasing amplitude, suggests that this is not purely scatter in the data (although that cannot be ruled out). Much the same can be said about the $\alpha_t = 14.1^\circ$, $\phi' = 45.4^\circ$ case.

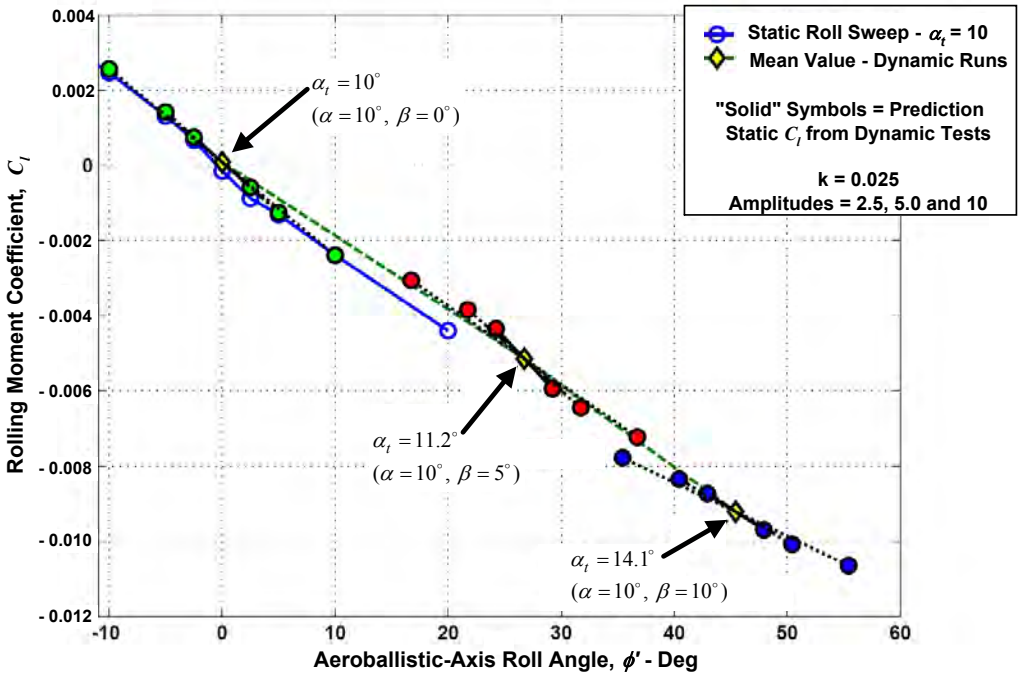

Figure 5-3 Amplitude Effects on "Static" Behavior

Frequency effects at these same three points are shown in Figure 5-4. In all these cases, the roll-angle amplitude was 2.5 degrees. Reduced frequencies of 0.025, 0.050, and 0.100 are plotted for all three cases. There is no clear trend (for the frequency effect) with increasing roll angle, and the "static" behavior is relatively independent of frequency.

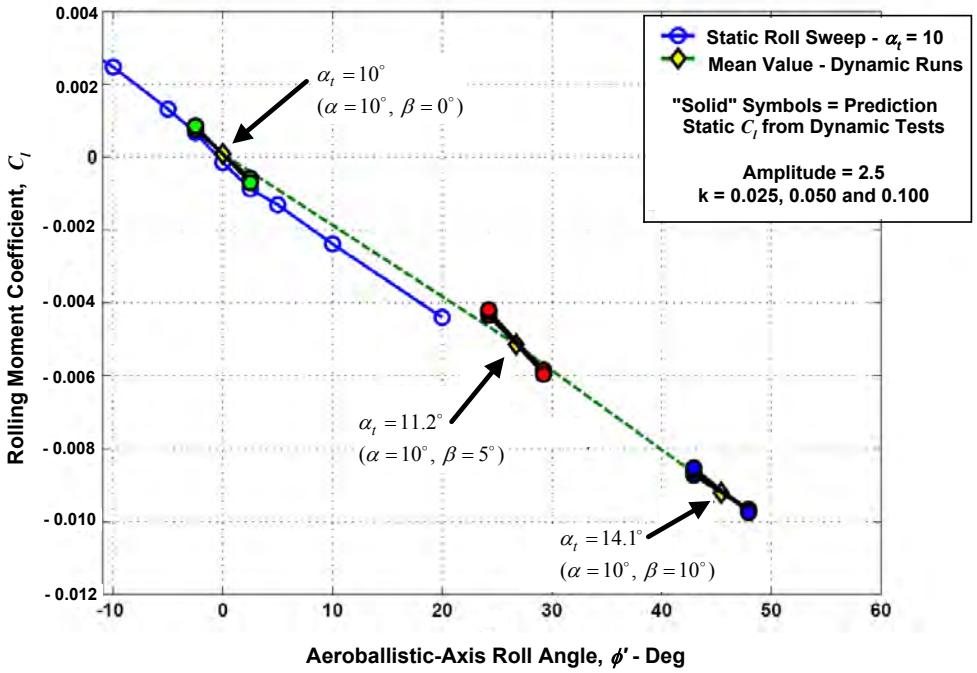

Figure 5-4 Frequency Effects on "Static" Behavior

Taken together these comparisons indicate that the stability derivatives will give reasonable results for small perturbations (about the reference flight condition), especially if the static derivatives are assumed to be nonlinear functions of α and β. However, we would expect quite different behavior for $\alpha_t > 10^\circ$ based on the roll sweep at 20 degrees (Figure 5-2). Those data indicate that the vehicle will experience an uncommanded roll to the left at $\beta = 0$ (because of the negative C_l there). Furthermore, the variation with roll angle is quite nonlinear and is not symmetric left to right. We should not assume that the conclusions reached above will apply here and all dynamic derivative data should be carefully checked.

Figure 5-5 presents data taken at $\alpha_t = 34^\circ$. Open blue points designate static data from a roll sweep. Again, the yellow diamonds represent the (interpolated) static rolling moment coefficient at mean roll angles of -7, -0.3, and 7 degrees respectively. The red, green and magenta "dumbbells" are the result from extrapolating the static derivatives (as determined from the dynamic test runs) over the roll-angle extremes reached during each run.

In all three cases, extrapolations at the lowest reduced frequency agree quite well with the static data. However, agreement degrades with increasing frequency. This is especially true for the dynamic run at a mean ϕ' of -0.3. This should raise a red flag, warning that a stability derivative model will not yield good results. Note again that the "static derivatives" extracted from a dynamic test are in fact the force/moment components that are in-phase with the motion. Under the conditions shown above, derivatives based on static tests are a poor approximation for this component.

The problem is similar to the case shown in Figure 2-8 where the dynamic derivatives are not unique in the 20 to 40 degrees angle of attack range. (Both of these cases are a result of the approximating the dynamic response by a simple lag). We can now be quite certain that under the conditions shown in Figure 5-5 the rolling moment response reacts very slowly to the changes in roll angle. Data at higher frequencies would be needed to determine if there is a fast-reacting component in the response. In that case, the "static" slope (determined dynamically) would approach a fixed value (other than zero) in the limit as the frequency gets very large; otherwise the dynamic response will simply approach the reference condition's mean static rolling moment coefficient.

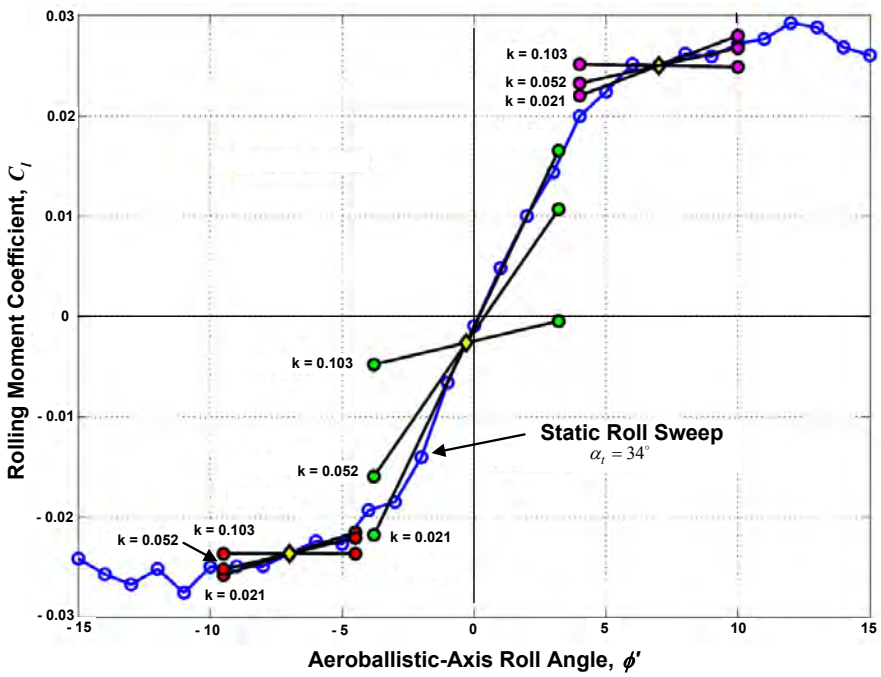

Figure 5-5 --Frequency Effects at $\alpha_t = 34^o$

5.3 Summary

The checks described above illustrate that when stability derivatives fail because the motion is too fast compared to the aerodynamic response, ***everything is dynamic***. There will always be a motion rate below which the stability derivatives give good results, i.e., the rate will be low enough that the linear terms of the asymptotic expansion is sufficiently accurate. ***However, if the vehicle motion rate ever exceeds that value, using the static derivatives*** **(as determined from static tests)** ***as an approximation for the "in-phase" part of the response will lead to significant errors*** (because the aircraft will not stay at any attitude relative to the air mass long enough for the aerodynamics to approach steady-state). Recall that acceleration "derivatives" depend on the static slope plus the time constant(s) of the indicial response: they approximate the lag in the aerodynamic response and are related to the area under the deficiency function. Therefore errors accrue when a simple lag is no longer sufficient to describe the physics of the problem. ***This point cannot be over emphasized.***

In the grand scheme of things, we may not mind missing the dynamic derivatives by 20% or more. However, errors in the "effective static derivatives" of that order are a source of great concern. Furthermore, ***we will never know if this is the case unless a dynamic test is conducted.***

6 Body Axis to Stability Axis Conversions

In the preceding discussions, all forces and moments were assumed to be the measured loads as seen by the balance. As such, they are body-axis "forces" since the balance is fixed relative to the model. Likewise, the model rotational motions were specified in the body-axis system. Often (even usually), stability derivatives are desired with respect to the so-called stability axes. Since stability axes are just a special case of a body-fixed axis system, the transformation for any single vector is straightforward. However, both the ***forces*** and the ***motions*** are to be expressed in the stability axis system since each derivative does in fact involve both a force/moment as well as a translational or rotational velocity. ***This is not a trivial complication.***

The difference between the two systems is that the x_{stab} axis is co-linear with the projection of the velocity vector (at the reference flight condition) onto the vehicle's plane of symmetry. The z_{stab} axis lies in the plane of symmetry and is, of course, perpendicular to the x axis. Therefore, a single rotation gets us from body axes to stability axes. This is a rotation about y_{body} and is equal to $-\alpha_0$.

Etkin[11] gives equations for transforming from one body-axis system to another. He does this for both the dimensional and nondimensional forms of the stability derivatives. By far the safest procedure is to perform the transformation on the dimensional derivatives, then nondimensionalize the result. This avoids complications brought about by the sometimes inconsistent use of reference quantities (by the U.S., U.K., and others).

Usually, the dimensional derivatives are defined with respect to the body-axis translational velocities (and accelerations) rather than the "aerodynamic angles." In this case, we may write

$$\begin{pmatrix}\Delta X\\ \Delta Y\\ \Delta Z\end{pmatrix}=\begin{pmatrix}X_u & 0 & X_w\\ 0 & Y_v & 0\\ Z_u & 0 & Z_w\end{pmatrix}\begin{pmatrix}\Delta u\\ \Delta v\\ \Delta w\end{pmatrix}+\begin{pmatrix}0 & X_q & 0\\ Y_p & 0 & Y_r\\ 0 & Z_q & 0\end{pmatrix}\begin{pmatrix}\Delta p\\ \Delta q\\ \Delta r\end{pmatrix}+\begin{pmatrix}X_{\dot u} & 0 & X_{\dot w}\\ 0 & Y_{\dot v} & 0\\ Z_{\dot u} & 0 & Z_{\dot w}\end{pmatrix}\begin{pmatrix}\Delta \dot u\\ \Delta \dot v\\ \Delta \dot w\end{pmatrix}$$

and

$$\begin{pmatrix}\Delta L\\ \Delta M\\ \Delta N\end{pmatrix}=\begin{pmatrix}0 & L_v & 0\\ M_u & 0 & M_w\\ 0 & N_v & 0\end{pmatrix}\begin{pmatrix}\Delta u\\ \Delta v\\ \Delta w\end{pmatrix}+\begin{pmatrix}L_p & 0 & L_r\\ 0 & M_q & 0\\ N_p & 0 & N_r\end{pmatrix}\begin{pmatrix}\Delta p\\ \Delta q\\ \Delta r\end{pmatrix}+\begin{pmatrix}0 & L_{\dot v} & 0\\ M_{\dot u} & 0 & M_{\dot w}\\ 0 & N_{\dot v} & 0\end{pmatrix}\begin{pmatrix}\Delta \dot u\\ \Delta \dot v\\ \Delta \dot w\end{pmatrix} \qquad 6\text{-}1$$

where:

ΔX, ΔY and ΔZ are the perturbations in force along the x, y, and z axes of the body-fixed coordinate system
ΔL, ΔM and ΔN are the moment perturbations about the x, y, and z axes of the body-fixed coordinate system

Note that Etkin has assumed that:

1. The derivatives of the lateral forces and moments with respect to the longitudinal state variables are zero.
2. The derivatives of the longitudinal forces and moments with respect to the lateral state variables can be neglected.
3. All derivatives with respect to the rates-of-change of the motion variables may be neglected except $X_{\dot u}$, $Z_{\dot u}$, $M_{\dot u}$, $X_{\dot w}$, $Z_{\dot w}$ and $M_{\dot w}$

We have included $Y_{\dot v}$, $L_{\dot v}$, and $N_{\dot v}$ for completeness. Of course any of the neglected terms can be reinstated (which may be wise depending on the configuration and flight conditions being examined). This could be especially important at high angles of attack and sideslip.

Derivative Transformations - Aerodynamic Angle to Velocity/Acceleration

The relationships given above (Equations 6-1) are expressed in terms of the body-axis velocity and acceleration perturbations. However, the equations of motion in stability axes are often written in terms of perturbations in α and β, therefore a procedure to account for this is needed. In addition, wind tunnel data is usually given in terms of α and β (or α_t and ϕ') and conversions are needed in order to put the aerodynamic data in the form required by Equations 6-1.

So, assuming that the body-axis static and acceleration derivatives with respect to α and β are known, the procedure is to first convert these into derivatives with respect to the body-axis velocity and/or acceleration components. These can then be transformed into stability-axis derivatives as detailed above. Finally, if desired, a conversion back to perturbations in α and β (in lieu of *u*, *v*, and *w*) can be made.

We begin with the matrix equations relating the body-axis state-variable perturbations to the stability derivatives in both forms, remembering that the total velocity (U_∞) is generally assumed to be a constant, e.g.,

$$\begin{pmatrix}\Delta X\\ \Delta Y\\ \Delta Z\end{pmatrix}=\begin{pmatrix}X_u & 0 & X_w\\ 0 & Y_v & 0\\ Z_u & 0 & Z_w\end{pmatrix}\begin{pmatrix}\Delta u\\ \Delta v\\ \Delta w\end{pmatrix} \quad \text{and} \quad \begin{pmatrix}\Delta X\\ \Delta Y\\ \Delta Z\end{pmatrix}=\begin{pmatrix}X_{U_\infty} & 0 & X_\alpha\\ 0 & Y_\beta & 0\\ Z_{U_\infty} & 0 & Z_\alpha\end{pmatrix}\begin{pmatrix}0\\ \Delta\beta\\ \Delta\alpha\end{pmatrix}$$

Of course these must be equal. However, we must be careful, the derivatives must be evaluated at the reference flight condition, i.e., with all perturbations set to zero. Equation 3-2 gives the body-axis velocity components in terms of α and β

$$\begin{pmatrix}u_b\\ v_b\\ w_b\end{pmatrix}=U_\infty\begin{pmatrix}\cos(\alpha)\cos(\beta)\\ \sin(\beta)\\ \sin(\alpha)\cos(\beta)\end{pmatrix}$$

Clearly, if β is held constant, a change in α requires both u_b and w_b to vary. A similar observation can be made regarding a varying β with α held constant. Therefore, variations in both α and β must be identified with ***the single velocity component*** responsible for the change. Because the aerodynamic system is assumed to be linear (for small perturbations), these effects can be superimposed, i.e., we may write

$$\Delta\alpha=\Delta\alpha_u+\Delta\alpha_w$$

and

$$\Delta\beta=\Delta\beta_u+\Delta\beta_v+\Delta\beta_w$$

However, due to assumptions 1 and 2 above, $\Delta\beta_u$ and $\Delta\beta_w$ can be disregarded because the stability derivatives associated with these have been neglected.

Therefore we have that

$$\begin{pmatrix}\Delta X\\ \Delta Y\\ \Delta Z\end{pmatrix}=\begin{pmatrix}X_u & 0 & X_w\\ 0 & Y_v & 0\\ Z_u & 0 & Z_w\end{pmatrix}\begin{pmatrix}\Delta u\\ \Delta v\\ \Delta w\end{pmatrix}=\begin{pmatrix}X_{U_\infty} & 0 & X_\alpha\\ 0 & Y_\beta & 0\\ Z_{U_\infty} & 0 & Z_\alpha\end{pmatrix}\begin{pmatrix}0\\ \Delta\beta_v\\ \Delta\alpha_u+\Delta\alpha_w\end{pmatrix} \qquad 6\text{-}2$$

All that remains is to relate $\Delta\beta_v$ to Δv, as well as $\Delta\alpha_u$ and $\Delta\alpha_w$ to Δu and Δw respectively. Take the angle-of-attack relationships first.

$$\alpha=\tan^{-1}\left(\frac{w}{u}\right)$$

Introducing the *u* perturbation

$$\tan\left(\Delta\alpha_u\right)\cong\Delta\alpha_u=\tan\left(\tan^{-1}\left(\frac{w}{u+\Delta u}\right)-\tan^{-1}\left(\frac{w}{u}\right)\right)$$

Linearization and the Equation 3-2 relationships give

$$\Delta\alpha_u=\frac{-w\,\Delta u}{u^2+w^2}=-\frac{\sin(\alpha_0)}{U_\infty\cos(\beta_0)}\Delta u$$

Similarly, for the perturbation in the *w*-velocity component we can show that to first order

$$\Delta\alpha_w=\frac{u\,\Delta w}{u^2+w^2}=\frac{\cos(\alpha_0)}{U_\infty\cos(\beta_0)}\Delta w$$

Finally, the sideslip perturbation due to Δv relationship follows directly from

$$\sin(\beta_0) = \frac{v}{U_\infty}$$

To first order, the change in β due to a perturbation in v (remembering that a perturbation in v, with u and w held constant, also changes U_∞) is given by

$$\Delta\beta_v = \frac{\cos(\beta_0)}{U_\infty}\Delta v$$

The derivative transformations follow from a straight-forward substitution into the scalar equations contained within Equation 6-2, taking the velocity/accelerations one at a time. For example, in the body-axis system we have:

$$X_u = \frac{\Delta\alpha_u}{\Delta u}X_\alpha = -\frac{\sin(\alpha_0)}{U_\infty\cos(\beta_0)}X_\alpha$$

$$Z_u = \frac{\Delta\alpha_u}{\Delta u}Z_\alpha = -\frac{\sin(\alpha_0)}{U_\infty\cos(\beta_0)}Z_\alpha$$

and

$$Y_v = \frac{\Delta\beta_v}{\Delta v}Y_\beta = \frac{\cos(\beta_0)}{U_\infty}Y_\beta$$

The remaining relationships are obtained in the same manner and are summarized in Tables Table 6-1through Table 6-4.

	X	***Y***	***Z***
u	$X_u = -\frac{\sin(\alpha_0)}{U_\infty\cos(\beta_0)}X_\alpha$	0	$Z_u = -\frac{\sin(\alpha_0)}{U_\infty\cos(\beta_0)}Z_\alpha$
v	0	$Y_v = \frac{\cos(\beta_0)Y_\beta}{U_\infty}$	0
w	$X_w = \frac{\cos(\alpha_0)}{U_\infty\cos(\beta_0)}X_\alpha$	0	$Z_w = \frac{\cos(\alpha_0)}{U_\infty\cos(\beta_0)}Z_\alpha$

Table 6-1 Static Force Derivative Conversions (Body Axes)

Note that the static and acceleration derivative conversions are identical.

	X	***Y***	***Z***
$\dot{u}$	$X_{\dot{u}} = -\frac{\sin(\alpha_0)}{U_\infty\cos(\beta_0)}X_{\dot{\alpha}}$	0	$Z_{\dot{u}} = -\frac{\sin(\alpha_0)}{U_\infty\cos(\beta_0)}Z_{\dot{\alpha}}$
$\dot{v}$	0	$Y_{\dot{v}} = \frac{\cos(\beta_0)Y_{\dot{\beta}}}{U_\infty}$	0
$\dot{w}$	$X_{\dot{w}} = \frac{\cos(\alpha_0)}{U_\infty\cos(\beta_0)}X_{\dot{\alpha}}$	0	$Z_{\dot{w}} = \frac{\cos(\alpha_0)}{U_\infty\cos(\beta_0)}Z_{\dot{\alpha}}$

Table 6-2 Force-Acceleration Derivative Conversions (Body Axes)

	L	***M***	***N***
u	0	$M_u = -\dfrac{\sin(\alpha_0)}{U_\infty \cos(\beta_0)} M_\alpha$	0
v	$L_v = \dfrac{\cos(\beta_0) L_\beta}{U_\infty}$	0	$N_v = \dfrac{\cos(\beta_0) N_\beta}{U_\infty}$
w	0	$M_w = \dfrac{\cos(\alpha_0)}{U_\infty \cos(\beta_0)} M_\alpha$	0

Table 6-3 Static Moment Derivative Conversions (Body Axes)

	L	***M***	***N***
$\dot{u}$	0	$M_{\dot{u}} = -\dfrac{\sin(\alpha_0)}{U_\infty \cos(\beta_0)} M_{\dot{\alpha}}$	0
$\dot{v}$	$L_{\dot{v}} = \dfrac{\cos(\beta_0)}{U_\infty} L_{\dot{\beta}}$	0	$N_{\dot{v}} = \dfrac{\cos(\beta_0)}{U_\infty} N_{\dot{\beta}}$
$\dot{w}$	0	$M_{\dot{w}} = \dfrac{\cos(\alpha_0)}{U_\infty \cos(\beta_0)} M_{\dot{\alpha}}$	0

Table 6-4 Moment-Acceleration Derivative Conversions (Body Axes)

Conversion from Body-Axis Derivatives to Stability-Axis Derivatives

To convert from a body-fixed system to stability axes, we premultiply the each derivative matrix by $\mathbf{L_2}(-\alpha_0)$, the matrix giving a rotation ($-\alpha_0$) about the y body-axis, and postmultiply by its transpose[10]. For example, consider the force-velocity derivatives.

$$\begin{pmatrix} X_{u_{stab}} & 0 & X_{w_{stab}} \\ 0 & Y_{v_{stab}} & 0 \\ Z_{u_{stab}} & 0 & Z_{w_{stab}} \end{pmatrix} = \underbrace{\begin{pmatrix} \cos(\alpha_0) & 0 & \sin(\alpha_0) \\ 0 & 1 & 0 \\ -\sin(\alpha_0) & 0 & \cos(\alpha_0) \end{pmatrix}}_{\mathbf{L_2}(-\alpha_0)} \begin{pmatrix} X_u & 0 & X_w \\ 0 & Y_v & 0 \\ Z_u & 0 & Z_w \end{pmatrix} \underbrace{\begin{pmatrix} \cos(\alpha_0) & 0 & -\sin(\alpha_0) \\ 0 & 1 & 0 \\ \sin(\alpha_0) & 0 & \cos(\alpha_0) \end{pmatrix}}_{\mathbf{L_2}^T(-\alpha_0) = \mathbf{L_2}(\alpha_0)}$$

Expansion of the RHS yields the following relations:

$$X_{u_{stab}} = \sin^2(\alpha_0) Z_w + \sin(\alpha_0)\cos(\alpha_0)\left(X_w + Z_u\right) + \cos^2(\alpha_0) X_u$$

$$X_{w_{stab}} = -\sin^2(\alpha_0) Z_u + \sin(\alpha_0)\cos(\alpha_0)\left(Z_w - X_u\right) + \cos^2(\alpha_0) X_w$$

$$Y_{v_{stab}} = Y_v$$

$$Z_{u_{stab}} = -\sin^2(\alpha_0) X_w + \sin(\alpha_0)\cos(\alpha_0)\left(Z_w - X_u\right) + \cos^2(\alpha_0) Z_u$$

$$Z_{w_{stab}} = \sin^2(\alpha_0) X_u - \sin(\alpha_0)\cos(\alpha_0)\left(X_w + Z_u\right) + \cos^2(\alpha_0) Z_w$$

These are summarized in Table 6-5.

Force / Moment Type	Stability-Axis Form	Coefficient of Transformation Equation			
		$\sin^2(\alpha_0)$	$\cos^2(\alpha_0)$	$\sin(\alpha_0)\cos(\alpha_0)$	1
Force – Velocity	$X_{u_{stab}}$	Z_w	X_u	$X_w + Z_u$	0
	$X_{w_{stab}}$	$-Z_u$	X_w	$Z_w - X_u$	0
	$Y_{v_{stab}}$	0	0	0	Y_v
	$Z_{u_{stab}}$	$-X_w$	Z_u	$Z_w - X_u$	0
	$Z_{w_{stab}}$	X_u	Z_w	$-X_w - Z_u$	0

Table 6-5 Body to Stability Axis Transformations (Force-Velocity)

However, substituting the body-axis ***force-angle derivatives*** for the force-velocity derivatives (using the relationships given in Table 6-1) leads to the simpler equations:

$$X_{u_{stab}} = Z_{u_{stab}} = 0$$

$$X_{w_{stab}} = \frac{\cos(\alpha_0) X_\alpha + \sin(\alpha_0) Z_\alpha}{U_\infty \cos(\beta_0)}$$

$$Y_{v_{stab}} = \frac{Y_\beta}{U_\infty \cos(\beta_0)} \qquad 6\text{-}3$$

$$Z_{w_{stab}} = \frac{\cos(\alpha_0) Z_\alpha - \sin(\alpha_0) X_\alpha}{U_\infty \cos(\beta_0)}$$

In the stability axis system, the relationships between the velocities and aerodynamic angles (to first order) are:

$$\Delta\alpha_w = \frac{\Delta w_{stab}}{U_\infty \cos(\beta_0)} \text{ and } \Delta\beta_v = \frac{\cos(\beta_0)}{U_\infty}\Delta v_{stab} \qquad 6\text{-}4$$

Note that the α perturbation in stability axes differs from its body-axis form because of the change in the "x" and "z" axis orientations relative to their body-axis positions. However, there is no change in the sideslip perturbation since the rotation is about the y-axis. We won't need the *u*-perturbation effect on angle of attack since the "*u*" derivatives are zero in stability axes. Furthermore, the symmetric perturbations on β can also be neglected for the reasons cited above.

Therefore, we can write the following expressions:

$$X_{\alpha_{stab}} = X_{w_{stab}} \frac{\Delta w_{stab}}{\Delta\alpha} = U_\infty \cos(\beta_0) X_{w_{stab}}$$

$$Y_{\beta_{stab}} = Y_{w_{stab}} \frac{\Delta v_{stab}}{\Delta\beta} = \frac{U_\infty}{\cos(\beta_0)} Y_{v_{stab}}$$

$$Z_{\alpha_{stab}} = Z_{w_{stab}} \frac{\Delta w_{stab}}{\Delta\alpha} = U_\infty \cos(\beta_0) Z_{w_{stab}}$$

Carrying this one step further by substituting for the velocity derivatives on the right hand side:

$$X_{\alpha_{stab}} = \cos(\alpha_0) X_\alpha + \sin(\alpha_0) Z_\alpha$$

$$Y_{\beta_{stab}} = Y_\beta$$

$$Z_{\alpha_{stab}} = \cos(\alpha_0) Z_\alpha - \sin(\alpha_0) X_\alpha$$

Perhaps these last three results should have been anticipated since a perturbation in angle of attack (or sideslip) produces the same effect regardless of coordinate system (leaving differences in the orientation of the forces between the two axis systems the only effect needing resolution).

Transformations of the moment-velocity derivatives result in quite different relationships because of the form of the moment-velocity derivative matrix. Note that there are two forces and one moment that are classified as longitudinal while the reverse is true in the lateral case. Furthermore, two of the velocity components are "longitudinal" and one is a lateral component. As a consequence of assumptions 1 and 2 above, the neglected "cross derivatives" appear in different locations in the moment-velocity derivative case.

That is we have for the moment-velocity derivatives:

$$\begin{pmatrix} 0 & L_{v_{stab}} & 0 \\ M_{u_{stab}} & 0 & M_{w_{stab}} \\ 0 & N_{v_{stab}} & 0 \end{pmatrix} = \begin{pmatrix} \cos(\alpha_0) & 0 & \sin(\alpha_0) \\ 0 & 1 & 0 \\ -\sin(\alpha_0) & 0 & \cos(\alpha_0) \end{pmatrix} \begin{pmatrix} 0 & L_v & 0 \\ M_u & 0 & M_w \\ 0 & N_v & 0 \end{pmatrix} \begin{pmatrix} \cos(\alpha_0) & 0 & -\sin(\alpha_0) \\ 0 & 1 & 0 \\ \sin(\alpha_0) & 0 & \cos(\alpha_0) \end{pmatrix}$$

An expansion of this matrix equation gives the relationships shown in Table 6-6.

Force / Moment Type	Stability-Axis Form	Coefficient of Transformation Equation	
		$\sin(\alpha_0)$	$\cos(\alpha_0)$
Moment - Velocity	$L_{v_{stab}}$	N_v	L_v
	$M_{u_{stab}}$	M_w	M_u
	$M_{w_{stab}}$	$-M_u$	M_w
	$N_{v_{stab}}$	$-L_v$	N_v

Table 6-6 Body to Stability Axis Transformations (Moment - Velocity)

Using the body-axis relationships defined in Table 6-3, equivalent conversions (in terms of the body-axis aerodynamic angles) are:

$$\begin{aligned} L_{v_{stab}} &= \frac{\cos(\beta_0)}{U_\infty}\left(N_\beta \sin(\alpha_0) + L_\beta \cos(\alpha_0)\right) \\ M_{u_{stab}} &= 0 \\ M_{w_{stab}} &= \frac{M_\alpha}{U_\infty \cos(\beta_0)} \\ N_{v_{stab}} &= \frac{\cos(\beta_0)}{U_\infty}\left(N_\beta \cos(\alpha_0) - L_\beta \sin(\alpha_0)\right) \end{aligned} \qquad 6\text{-}5$$

Finally a conversion to the stability-axis derivatives with respect to the aerodynamic angles, using Equations 6-4 yields:

$$\begin{aligned} L_{\beta_{stab}} &= N_\beta \sin(\alpha_0) + L_\beta \cos(\alpha_0) \\ M_{\alpha_{stab}} &= M_\alpha \\ N_{\beta_{stab}} &= N_\beta \cos(\alpha_0) - L_\beta \sin(\alpha_0) \end{aligned}$$

Most often body-axis static force and moment derivatives with respect to α and β will be directly available from a static test (seldom are conversions to derivatives with respect to the translational velocities provided as output). Therefore, if stability-axis derivatives with respect to velocities are desired, Equations 6-3 and 6-5 are most convenient.

Rotational Derivative Conversions

Consider now the rotational derivatives of the aerodynamic moments.

$$\begin{pmatrix} L_{p\,stab} & 0 & L_{r\,stab} \\ 0 & M_{q\,stab} & 0 \\ N_{p\,stab} & 0 & N_{r\,stab} \end{pmatrix} = \begin{pmatrix} \cos(\alpha_0) & 0 & \sin(\alpha_0) \\ 0 & 1 & 0 \\ -\sin(\alpha_0) & 0 & \cos(\alpha_0) \end{pmatrix} \begin{pmatrix} L_p & 0 & L_r \\ 0 & M_q & 0 \\ N_p & 0 & N_r \end{pmatrix} \begin{pmatrix} \cos(\alpha_0) & 0 & -\sin(\alpha_0) \\ 0 & 1 & 0 \\ \sin(\alpha_0) & 0 & \cos(\alpha_0) \end{pmatrix}$$

Expansion of the RHS yields the following relations:

$$L_{p\,stab} = \sin^2(\alpha_0)N_r + \sin(\alpha_0)\cos(\alpha_0)\left(L_r + N_p\right) + \cos^2(\alpha_0)L_p$$

$$L_{r\,stab} = -\sin^2(\alpha_0)N_p + \sin(\alpha_0)\cos(\alpha_0)\left(N_r - L_p\right) + \cos^2(\alpha_0)L_r$$

$$N_{p\,stab} = -\sin^2(\alpha_0)L_r + \sin(\alpha_0)\cos(\alpha_0)\left(N_r - L_p\right) + \cos^2(\alpha_0)N_p$$

$$N_{r\,stab} = \sin^2(\alpha_0)L_p - \sin(\alpha_0)\cos(\alpha_0)\left(L_r + N_p\right) + \cos^2(\alpha_0)N_r$$

Note that conversions for the rotary derivatives of the aerodynamic moments parallel those for the force-velocity derivatives because the elements of the column vector of rotational perturbations (Δp, Δq, Δr) are "lateral, longitudinal, lateral," in that order, while the sequence of moments (L, M, N) is the same. This forces the ***off-diagonal elements*** of the derivative matrix to be zero since these positions correspond to cross derivatives.

Force / Moment Type	Stability-Axis Form	Coefficient of Transformation Equation			
		$\sin^2(\alpha_0)$	$\cos^2(\alpha_0)$	$\sin(\alpha_0)\cos(\alpha_0)$	1
Moment - Rotary	$L_{p\,stab}$	N_r	L_p	$L_r + N_p$	0
	$L_{r\,stab}$	$-N_p$	L_r	$N_r - L_P$	0
	$M_{q\,stab}$	0	0	0	M_q
	$N_{p\,stab}$	$-L_r$	N_p	$N_r - L_p$	0
	$N_{r\,stab}$	L_p	N_r	$-L_r - N_P$	0

Table 6-7 Body to Stability Axis Transformations (Moment - Rotary)

Note especially, that the conversions require knowledge of the body-axis yawing-moment and rolling-moment rotational derivatives with respect to both yaw-rate ***and*** roll-rate. Thus, two dynamic test blocks (for body-axis roll and yaw rate motions) are required to transform to equivalent stability axis derivatives. The fact that single degree-of-freedom rotational tests are "contaminated" with acceleration derivative responses makes these conversions more problematic. No conversion is needed for the pitch-damping derivative M_q.

Force / Moment Type	Stability-Axis Form	Coefficient of Transformation Equation	
		$\sin(\alpha_0)$	$\cos(\alpha_0)$
Force - Rotary	$X_{q\,stab}$	Z_q	X_q
	$Y_{p\,stab}$	Y_r	Y_p
	$Y_{r\,stab}$	$-Y_p$	Y_r
	$Z_{q\,stab}$	$-X_q$	Z_q

Table 6-8 Body to Stability Axis Transformations (Force - Rotary)

Not surprisingly then, the form of the moment-velocity derivative conversions mimics the force-velocity conversions because the diagonal elements in both of these cases contain the cross derivatives.

References

[1] Tobak, M., and Schiff, L. B., "Aerodynamic Mathematical Modeling – Basic Concepts," *AGARD Symposium on Unsteady Aerodynamics – Fundamentals and Application to Aircraft Dynamics*, 1985, AGARD CP-386.

[2] Bryan, G. H., *Stability in Aviation*, 1911, Macmillan and Co., London.

[3] Kuethe, A. M. and Schetzer, J. D., *Foundations of Aerodynamics, Second Edition*, John Wiley & Sons, 1967, Appendix A

[4] Etkin, B., "The Linear Air Reactions," *Dynamics of Atmospheric Flight*, 2005, Dover Publications, Inc., New York, pp. 158-160.

[5] Fung, Y.C., Sections 6.1, 6.2, and 6.7, *An Introduction to the Theory of Aeroelasticity*, 1969, Dover Publications, Inc., New York, pp. 187-193 and 206-210.

[6] Etkin, B., "Superposition Theorem," *Dynamics of Atmospheric Flight*, 2005, Dover Publications, Inc., New York, pp. 89-93.

[7] Brandon, Jay M., et al, "Comparison of Rolling Moment Characteristics During Roll Oscillations for a Low and a High Aspect Ratio Configuration, AIAA Paper 2004-5273, Aug. 2004.

[8] Etkin, B., "Representation by Transfer Functions," *Dynamics of Atmospheric Flight*, 2005, Dover Publications, Inc., New York, p. 166.

[9] Etkin, B., "Frequency Response," *Dynamics of Atmospheric Flight*, 2005, Dover Publications, Inc., pp. 78-81.

[10] Etkin, B., "Reference Frames and Transformations," *Dynamics of Atmospheric Flight*, 2005, Dover Publications, Inc., New York, pp. 104-120.

[11] Etkin, B., "General equations of unsteady motion", *Dynamics of Atmospheric Flight*, 2005, Dover Publications, Inc., pp. 191-195.